How Dissipation Constrains Fluctuations in Nonequilibrium Liquids: Diffusion, Structure, and Biased Interactions

Laura Tociu^{1,2} Étienne Fodo³, Takahiro Nemoto⁴, and Suriyanarayanan Vaikuntanath²an ¹James Franck InstituteUniversity of Chicago, Chicago, Illinois 60637, USA ²Department of Chemistry, University of Chicago, Chicago, Illinois 60637, USA ³DAMTP. Centre for MathematicaSciencesUniversity of Cambridge, Wilberforce Road, Cambridge CB3 0WAUnited Kingdom ⁴Philippe Meyer Institute for TheoreticaPhysics,Physics DepartmentĘcole Normale Su**e**rîeure and

PSL Research Universit/24, rue Lhomond,75231 Paris Cedex 05France

(Received 15 October 2018evised manuscript received 15 September 2019; published 5 November 2019)

The dynamics and structure of nonequilibrium liquids, driven by nonconservative forces which can be either external or internal, generically hold the signature of the net dissipation of energy in the thermostat. Yet, disentangling precisely how dissipation changes collective effects remains challenging in many-body systems due to the complex interplay between driving and particle interactions. First, we combine explicit coarse-graining and stochastic calculus to obtain simple relations between diffusion, density correlations, and dissipation in nonequilibrium liquidsBased on these resultswe considerlarge-deviation biased ensembles where trajectories mimic the effect of an external drive. The choice of the biasing function is informed by the connection between dissipation and structure derived in the first part. Using analytical and computationaltechniques,we show that biasing trajectories effectively renormalizes interactions in a controlled mannerthus providing intuition on how driving forces can lead to spatialrganization and collective dynamicsAltogether, our results show how tuning dissipation provides a route to alter the structure and dynamics of liquids and softaterials.

DOI: 10.1103/PhysRevX.9.041026

Subject Areas: Chemical Physics Soft Matter, StatisticalPhysics

I. INTRODUCTION

Nonequilibrium forces can drive novel and specific in materials. The close connection between the netlissipation of energy, powered by these forces, internal transport, and spatial organization is especially apparent in living systems [1-4]. As an example, the flagella motor of Escherichia coli exhibit a unique phenomenology combining ultrasensitive responsedaptation and motor restructuring as a function of the applied load [5–7]. Moreover, in vivo studies of the cellular cytoskeletonas show that motor-induced forces control large variety of functionality in the cell [8-12].

To elucidate the role of nonequilibrium forces in materials, it is crucial to examine how dissipation affects the emerging dynamics and structure. While equilibrium

Published by the American Physical Society under the terms of the Creative Commons Attribution 4.0 International license. Further distribution of this work must maintain attribution to the author(s) and the published article's titlejournal citation, and DOI.

features are well established, progress in controlling systems with sustained dissipation is hampered by a lack of general pathways to modulate phase transitions and self-assembly and driven systems provide analytically and numerically tractable test beds to investigate the interplay between dissipation and material properties far from equilibrium [20–24]. They illustrate, for instance, how nonequilibrium Striving can induce phase transitions and excite novel collective responses in softmedia [15,21,25-27].Recent theoretical work proposes extending equilibrium concepts to active media, such as the definition of pressure [14,28], to rationalize their phenomenology [29,30]Others strive to well as in vitro experiments on reconstituted systems, alsobtain stationary properties of active matter through perturbation close to equilibrium [16,31,32], inspired by other approaches on driven systems [33–36].

> To investigate how dissipation controls emerging behavior, yet another approach focuses on introducing a bias in dynamical ensembles. Using large-deviation techniques, trajectories are conditioned to promote atypical realizations of the dynamics [37,38]. Such techniques are used for instance, to investigate the role of dynamical heterogeneities in glassy systems [39–45] and soliton solutions in high-dimensional chaotic chains [46,47]. More recently, it has been shown that changing dissipation, through a dynamical bias strongly affects the internal transport and

the density fluctuations of nonequilibrium liquids [48,49], [46,63–68], we show that biased sampling trajectories thus confirming that controlling dissipation is indeed a fruitful route to tailoring material properties. In spite of these advancesanticipating the emergentlynamics and structure of biased nonequilibrium systems is stillchallenging in the presence of many-body interactions [38,50]noise realizations can then serve as proxies of how to so that precise control has remained elusive so far in this control the dynamics by applying an externaforce with context. Consequently any generic principle rationalizing spatial organization in terms of dissipation is still lacking.

In this paper, we explore how dissipation affects the First, we consider in Sec. II two types of assemblies of Brownian particles: one in which only a subset is driven by groundwork for precise controb the emerging structure experience an internal active force. We first focus on instances where the fraction of driven particles is less than the fraction of undriven particles, so that driven and undriven particles are respectively referred to as tracer and bath particles. Using the diffusion coefficient of a tracer and bath particlesve connect dissipation to liquid properties. In contrast to Ref. [23], our prediction for diffusion follows from a systematic coarse graining with explicit dependencein terms of microscopic details [51-53].

Next, importantly, we put forward a generic relation between density correlations and dissipation valid for an arbitrary driving force: This relation is our first main result where $\delta_{i\in\Omega}$ 1/4 1 if $i\in\Omega$ and $\delta_{i\in\Omega}$ 1/4 0 otherwise. The We demonstrate thathis result holds both for fluids in which a fraction of the particles are driven by a fixed external drive and for fluids in which either a fraction of the a zero-mean Gaussian white noise with correlations liquid or the entire liquid is driven by an internal noise, analogousto the driving used in model active matter systems. This result opens the door to estimating dissipation directly from the liquid structure, in contrast to previous approaches based either on perturbing the system [54–58] or on analyzing trajectories and currents in phase space [3,59-62]. We illustrate this result with numerical simulations for which dissipation is quantified by the deviation from equilibrium tracer-bath correlations. Using these results as a basise also show how various aspects of the pair correlation function of a nonequilibrium protocol given in two dimensions by liquid are effectively constrained by the energy dissipation. Altogether, this set of results clarifies how nonequilibrium forces affect the transport and structure of the liquid, thus showing how liquid properties can be modified at the costwhere f and ω are, respectively the amplitude and the of energy dissipation.

Motivated by these results, and to provide concrete intuition for how particular configurations can be stabilize Φ clet number Pe $\frac{1}{2}$ σ f=Twhere σ is the typical particle by nonequilibrium forces, we next investigate in Sec. III the ize [21,23]. In the absence of interactions (v ¼ 0), the emerging structure of Brownian particles subject to a dynamicalbias. The explicit form of the bias is inspired by the results of Sec.II connecting dissipation to manybody interactions. Using analytical calculations and numerical simulations based on the cloning algorithm

can be used to renormalize any specific interparticle interaction in a multicomponent liquid. The rare noise fluctuations sampled with dynamical bias effectively drive the system away from typicabehavior [38-45,50]. Such complex protocols. We also illustrate the generality of our ideas by considering an assembly of aligning self-propelled particles [69]. Specifically, we show how biased energy dynamics and structure of many-body diffusive systems. flows can renormalize interactions between particles and stabilize a flocking transition. Overall, our results lay the an external force and one in which a subset of the particles and collective dynamics in many-body diffusive nonequilibrium systems.

II. DISSIPATION AND LIQUID PROPERTIES

In this section, we provide a series of relations between tagged tracer particle and the density correlations between energy dissipation and liquid properties in nonequilibrium liquids. Specifically, we consider interacting Brownian particles where a specific set Ω particles Ω is driven by a nonconservative force F:

$$\gamma_{\Gamma_{i}} \stackrel{\mathcal{H}}{\sim} \delta_{\in \Omega} F_{d;i} - \nabla_{i} \quad \text{v\'{o}} r_{i} - r_{j} \triangleright \beta \xi;$$
 \check{o} 1

driven particles belonging to the seΩ are referred to as tracers and others as bath particles. The fluctuating term ξ ȟξ_αðtÞϜೄð0Þi ¼ 2γΤρδαβδðtÞ,where γ and Τ, respectively, denote the damping coefficient and the bath temperature, with the Boltzmann constant set to unity (k1/4 1).

A. Deterministic vs active drive

In what follows, we consider two types of drive: (i) an external force following the same deterministic protocol for all driven particles and (ii) an internal force given by a noise term independentfor each driven particle. Building on recent work [21,23], we take for drive (i) a time-periodic

$$F_d \delta t \triangleright \frac{1}{4} f \frac{1}{2} \sin \delta \hat{u} \hat{e} t \triangleright \cos \delta \omega t \hat{e}_v; \qquad \delta 2 \triangleright$$

frequency of the drive so that the drive persistence reads $\tau \frac{1}{4} 2\pi = \omega$. The relative strength of the drive is given by the average position of driven tracers follows a periodic orbit, describing a circle in two dimensions. In contrast, drive (ii) corresponds to a random self-propulsion as is often considered in active liquids [70–72]. Specifically, we use a set of zero-mean Gaussian noises with correlations

$$hF_{d;i\alpha}\delta t P_{d;j\beta} \delta 0 Pi \ 1/4 \ \ \, \ \, \delta \alpha \beta \frac{f^2}{d} e^{-jtj=\tau} \, ; \qquad \qquad \delta 3 P$$

where d is the spatial dimension. The parameters f and τ, respectively control the amplitude and the persistence of fluctuations.

Interestingly, the active force with correlations (3) can be obtained from a generalized version of the deterministic force (2) where each particle i is now subjected to an independent drive. The period of the orbit is determined by a series of n oscillators with identical frequencies for all particles yet independent mplitudes:

to implement disorder in the drive, which is done by taking nduced phase separation of active particles [13,36] pulation the oscillator amplitudes as uncorrelated zero-mean Gaussian variables with unit variance:

$$hA_{ai\alpha}A_{bi\beta}i_d \frac{1}{4}\delta_{ab}\delta_{ij}\delta_{\alpha\beta} \frac{1}{4}hB_{ai\alpha}B_{bi\beta}i_d;$$
 ð5Þ

where his denotes an average over the disorder. It follows deterministic set of equations. that F_{d:i} is also a Gaussian process with zero mean and correlations given by

$$hF_{d;i\alpha}\delta t PF_{d;j\beta}\delta 0 P_{d} \stackrel{1}{\sim} \chi_{0j} \delta_{\alpha\beta} \frac{f^2}{nd} \frac{X^n}{nd} \cos \delta_{\omega} t P$$
: $\delta 6 P$

In the limit of a large number of oscillators ($n \gg 1$),we frequencies φ as

$$hF_{d;i\alpha} \delta t \triangleright F_{d;j\beta} \delta 0 \triangleright i \frac{1/4}{n \gg 1} \delta_{ij} \delta_{\alpha\beta} \frac{f^2}{d}$$
 $\phi \delta \omega \triangleright e^{i\omega^0 t i} \frac{d\omega^0}{2\pi}$: $\delta 7 \triangleright i$

This expression establisheshat, in the limit of many oscillators, the deterministic drive (4) with disordered amplitude is equivalento a noise term with spectrum φ. In particular, by choosing φδωρ ¼ 2τ=½1 þ δωρ², the drive correlations (7) reproduce exactly the ones of the random force in Eq.(3).

numerically the many-body dynamics (1) where every particle is subjected to a disordered drive of the form (4). We use the potential vorb ¼on - jrj=σβoo - jrjb, where Θ denotes the Heaviside step functiowhich sets purely repulsive interactions. To implement numerically the disorder in driving, it is sufficient to sample the amplitudes fA ai; Baig and frequencies fug at the initial time. In the

regime of high persistence τ and large average density ρ where KðrÞ ¼ δðrÞπ p vðrÞ=T. Note that density flucwe observe the spontaneous formation of clusters up to atuations remain generally Gaussian even for a homocomplete formation at a large time; see Fig. 1. This formation is analogous to the motility-induced phase

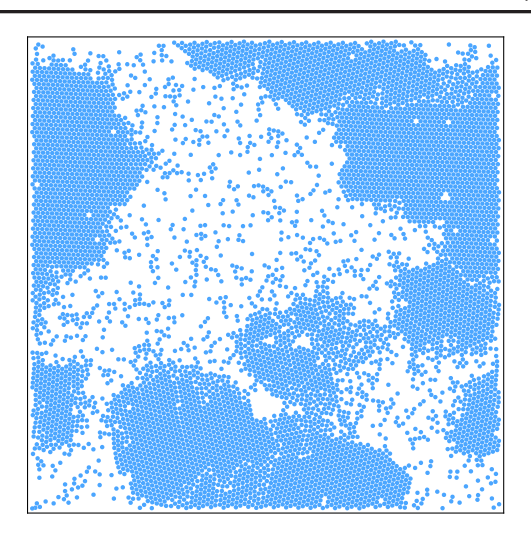


FIG. 1. Snapshot of particles subjected to a disordered drive. A The essential ingredient of the mapping into active force is hase separation emerges which is analogous to the motilitydetails are in the Appendix A and the movie in Re[73].

separation commonly reported in standard models of active particles [13,26]. Interestingly, it appears in our case even in the absence of fluctuations (T $\frac{1}{4}$ 0), namely, for a purely

In short, we thus demonstrate that the disordered drive alone reproduces the emerging physics of active systems. This important result bridges the gap between two main classes of nonequilibrium liquids, where the driving force stems from either a deterministic protocol or a random noise. In what follows, we obtain analytic and numerical results for both drives to illustrate the broad applicability of express these correlations in terms of the density of drivingur framework, ranging from systems driven by deterministic fields to active matter systems.

B. Dissipation controls tracer diffusion

To connect tracer diffusion with dissipation, we first describe the dynamics of undriven particles in terms of a coarse-grained variableUsing standard techniques, the dynamics of the density field ρðr; tÞ ¼ i∈Ω δ½r - iðtÞ can be written as a nonlinear Langevin equation [51]. In the regime of weak interactions, the density fluctuations δρδr; tÞ ¼ pðr; tÞ ¬ paround the average density ρ are To illustrate the relevance of this mapping, we simulateGaussian and captured by the following Hamiltonian [53,74,75]:

geneous active liquid [70]. The conserved density dynamics reads

$$\begin{split} \frac{\partial \delta \rho \delta r; \, t P}{\partial t} & \frac{Z}{4} \, D_G \nabla^2 & \text{K\'or} - r^0 P \delta \rho \delta f; \, t P d P \\ & p \, \frac{1}{Y_G} \nabla^2 & \text{V\'a}_i \delta t P - f \delta t P \mid \nabla \cdot \Lambda \delta r; \, t P; \quad \delta 9 P \end{split}$$

where $D_G \frac{1}{4} \rho_0 T = \gamma$ and $\gamma_G \frac{1}{4} \gamma = \rho_0$ are, respectively,the field diffusion coefficient and the field damping coefficient. J $\frac{1}{4}$ Nf 2 = $\gamma - \underline{w}$, where the rate of work reads The term Λ is a zero-mean Gaussian white noise with correlations hhôr;tÞ/hðr⁰,t⁰Þi¹/₄2D_Gδ_{αβ}δðr-r ⁰Þδðt-fÞ.

Owing to the linearity of the density dynamics (9), it can be readily written in Fourier space δρδq; tÞ 1/4 ρðr; tÞē^{iq⋅r} dr as

$$\begin{split} \frac{\partial \delta \rho \delta q; \ tP}{\partial t} &\frac{1}{4} - jqj^2 D_G K \delta q P \delta \rho \delta q; \ tP \\ &- jqj^2 \frac{v \delta q P^{X}}{\gamma_{G_{-i \in O}}} e^{-iq \cdot r_{-j} \delta t P} p \ iq \cdot \Lambda \delta q; \ tP; \quad \delta 10 P \end{split}$$

so that the field dynamics can be directly solved as

$$\begin{array}{c} Z\\ \delta\rho\delta q;\ t \vdash \frac{1}{4} \int_{-\infty}^{t} ds e^{-D_G jqj^2 K \delta q \vdash \delta t - s \vdash} \\ \times \quad iq \cdot \Lambda \delta q;\ s \vdash - jq_1^2 \frac{v \delta q \vdash^X}{\gamma_G} \int_{j \in \Omega}^{t} e^{-iq \cdot r_j \, \delta s \vdash} : \quad \delta 11 \vdash t = 0 \end{array}$$

Considering the limit of dilute driven tracers, where interactions among them are negligible, their dynamics reads

 $\frac{R}{a}$ $\frac{R}{4}$ $\frac{R}{dq}$ $\frac{8}{4}$ $\frac{8}{4}$ $\frac{8}{4}$ $\frac{1}{4}$ $\frac{1$ provide closed time-evolution equations for tracers only. It should be valid only for weak interactions a priori, yet previous works show that it remains qualitatively relevant even beyond this regime in practice [76–78]. Indeed, Gaussian field theories for density fluctuations provide a very good description of simple liquids [74].

To characterize the transport properties of the liquid in the presence of driving forces, our first goal is to obtain an explicit expression, in terms of microscopic details, for the tracer diffusion coefficient:

D
$$\frac{1}{4} \lim_{t \to \infty} \frac{1}{2dt} h \frac{1}{2} h t = r_i \delta t$$

which is defined from stochastic thermodynamics as the power of the forces exerted by all tracers on solvent: , hr. · ðyr. - ξ, Þi, where · denotesa Stratonovich product[79,80]. Dissipation is directly related to entropy production, as a measure of irreversibility both when the

drive is deterministic [79,80] and when it is a correlated noise [81-84]. Substituting the dynamics (1) the dissipation soincides with the power of driving forces: $_{i\in\Omega}$ h_{T_i} · $F_{d;i}$ i. Besides,replacing f_i by its expression in Eq. (1) and using the fact that ξ_i and F_{di} are uncorrelated, we deduce that the dissipation can be further separated into free-motion and interaction contributions as

$$\underline{\mathbf{w}} \stackrel{1}{\cancel{4}} \frac{1}{\mathbf{Y}} \mathbf{h} \mathbf{F}_{d;i} \cdot \nabla_{i} \mathbf{v} \delta \mathbf{r}_{i} - \mathbf{r}_{j} \mathbf{b} \mathbf{i} : \qquad \delta 14 \mathbf{b}$$

Given that w is the only nontrivial contribution to dissipation, connecting diffusion and dissipation simply amounts to expressing D in terms of.

Deriving transport coefficients in nonequilibrium manybody systems, whose collective effects result from the complex interplay between interaction and driving forces, is a notoriously difficult task [85–89]. We set up a proper perturbation scheme by scaling the pair potential v with a small dimensionless parameter $h \ll 1$ which controls the coupling between tracerand bath. In Appendix B, we obtain some explicit expressions for D and to quadratic order in h and in the scaled driving amplitude Pe.

First, we discuss the case of the deterministic drive (2), and we focus on the limits of small and large driving frequency, respectively $\omega \tau_r \ll 1$ and $\omega \tau_r \gg 1$, where the relaxation timescale τ¼ δD_G=σ²ÞKðjqj ¼ 1=σÞ is setty density diffusion over the tracer size σ. First, at high frequencies ωτ≫ 1, the rate of work per particle N and the deviation from equilibrium diffusion D - Dea, where D_{eq} is the diffusion coefficient for Pe ½ 0, are given, respectivelyby

It
$$\frac{W}{N} \frac{1}{4} \frac{hPe}{\omega}^2 \cdot \frac{\delta T = \sigma \beta}{d\gamma^3}^Z \frac{1}{q} jqj^4jv\delta qP_f^2 \frac{1}{k} \frac{p}{k} \frac{p}{k} \frac{p}{k}$$
;
 $D - D_{eq} \frac{1}{4} \frac{hPe}{\omega}^2 \cdot \frac{T = \sigma^2}{d\gamma^3}^Z \frac{jqj^2jv\delta qP_f^2}{k\delta qP^{1/2} 1} \frac{1}{p} \frac{p}{k} \frac{k\delta qP}{k}$: $\delta 15P$

In the opposite limit of low frequencies $\omega_{\overline{I}} \ll 1$, we get

$$\begin{split} &\frac{\underline{w}}{N} \frac{1}{4} \frac{\eth h P e^{\beta}}{d \gamma \sigma^2} \frac{Z}{q} \frac{j v \eth q P_f^2}{K \eth q P_{2}^{1/2} 1 \ p_0 \cancel{k} \eth q P}; \\ D - D_{eq} \frac{1}{4} \frac{5 \eth h P e^{\beta}}{d \gamma T \sigma^2} \frac{j v \eth q P_f^2}{q} \frac{j v \eth q P_f^2}{j q j^2 K \eth q P_{2}^{1/2} 1 \ p_0 \cancel{k} \eth q P^3}; \quad \eth 16 P_{2} \end{matrix}$$

We aim to explore connections between D and dissipation both w=N and D - Qa are now independent of the driving frequency ω . As a result, our perturbation theory shows that the scalings of and D - \mathbf{D}_{eq} are identical, in terms both of the drive amplitude Pe and of its frequency ω, in asymptotic frequency regimes. Note that the scaled rate of work w=ðNf²Þ coincides with the reduced equilibrium diffusion

 γD_{eq} =T - 1 to this order [52,53],as expected from linear response.

by using the mapping between the disordered drive and active forcing in SecJI A. In practice, we first derive the diffusion coefficient D and the rate of work w for the driving force (4) at fixed disorder, as a straightforward generalization of the deterministic driving case and we then average over the disorder. At small persistence, $\tau \ll r$ ate at which the potential U $\frac{1}{4}$ $_{i \in \Omega; j}$ v $\delta r_i - r_j \triangleright$ changes, we get

$$\frac{\underline{w}}{N} \frac{1}{4} \frac{\tau T \delta h P e^{\beta}}{d \delta \sigma \gamma \beta}^{Z} \frac{j q j^{2} j v \delta q P_{f}^{2}}{K \delta q P};$$

$$D - D_{eq} \frac{1}{4} \frac{3 \tau \delta h P e^{\beta}}{d \delta \sigma \gamma \beta}^{Z} \frac{j v \delta q P_{f}^{2}}{K \delta q P^{2} 2 1 p_{0} K \delta q P^{2}}; \qquad \delta 17 P$$

In contrast, the large persistence limit $\gg \tau_r$ yields the same results as forthe low-frequencies regime ofdeterministic drive, namely, the expressions (16) Indeed, the force F_{d:i} has a constant direction in such a limit, and the difference between deterministic and active drives, which, respectively correspond to independent similar directions for each tracer, is irrelevant in the limit of dilute tracers.

When the size a of the bath particles is significantly smaller than the tracer size $\sigma \gg a$, which amounts to setting defined in Eq. (14) and the term $\underline{w}_{AC} \%$ $f_{i;jg=\Omega}$ $hF_{d;i}$ different pair potentials v for bath-bath and for bath-tracer vor i vor interinteractions, one can safely neglect the variation of Koqb interactions among driven particles to dissipationThe latter regimes $\omega \tau_r \gg 1 (\tau \ll \tau_r)$ and $\omega \tau_r \ll 1 (\tau \gg \tau_r)$, the renormalization of the diffusion coefficient D - Deq can be simply written in terms of the rate of work per particle w=N for Pe ≪ 1 as

$$\frac{D - D_{eq}}{\sigma^2} \sim \frac{\underline{W}}{NT}$$
: ð18Þ

Thus, the excess rate at which tracers move over their own size compared to equilibrium, set by the lhs of Eq. (18), is controlled by the rate at which work is applied on tracers by nonequilibrium forces, set by the rhs of Eq. (18). The proportionality factor depends on the details of interactions and of density fluctuations. Interestingly, this result is valid where for both deterministic and active drives. It corroborates numerical observations obtained previously in a system where composition-dependent diffusion constants can lead to phase transitions [23].

C. Dissipation sets density correlations

correlations of the liquid. To this end, we treat undriven bath particles without any approximation in what follows, instead of relying on the Gaussian density field theory for and $^{\circ}$ denotes a sum without the overlap of indices: i \neq j, δρ as in Sec. II B, and we consider an arbitrary set of

driving forces F_{d:i}. In equilibrium, the liquid structure can be derived from a hierarchy of equations for density The case of the active drive with correlations (3) followscorrelations, whose explicit form reflects the steady-state condition on the many-body distribution function [90]n our settings, steady-state conditions should now provide modified equations for density correlations, which can potentially make apparent the connection with dissipation.

> This observation motivates us to consider the average which can be written using Itô calculus as

γΗJi ¼
$$h^{1/2}$$
γρ̄ – $\underline{r_j}$ Þ þ $2T\nabla_i \cdot \nabla_i$ vð r_i – r_j Þi: ð19Þ

Substituting the dynamics (1) and using $h\xi_i \cdot \nabla_i vi \frac{1}{4} 0$ within the Itô convention, we get

In the first line of Eq. (20), we recognize the rate of work Eqs. (15)–(17), so that KôqÞ ~ Kôjqj ¼ 1=aÞ. Then, in bothanishes exactly when the drive is identical for all particles, since $\int_{\text{fi;ig} \in \Omega} \nabla_i v \delta r_i - r_j \triangleright \frac{1}{4} 0$ by symmetry, and it can be neglected for an active drive when the fraction of driven particles is small. Then, using the steady-state condition hUi 1/4 0, we deduce

The both deterministic and active drives. It corroborates sumerical observations obtained previously in a system
$$g\delta r \triangleright \frac{1}{N} h\delta \delta r - i r \rho r_j \triangleright i;$$
 here composition-dependent diffusion constants can lead sphase transitions [23].
$$g_{3a}\delta r; h \triangleright \frac{1}{N^2} \sum_{i \in \Omega; j; k} h\delta \delta r - i r \rho r_j \triangleright \delta \delta h - r_i \rho r_k \triangleright i;$$
 C. Dissipation sets density correlations

We now explore how dissipation relates to static density $g_{3b}\delta r; h \triangleright \frac{1}{N^2} \int_{i \in \Omega; j; k} h\delta \delta r - i r \rho r_j \triangleright \delta \delta h - r_j \rho r_k \triangleright i;$ $\delta 22 \triangleright 0$ formulations of the liquid. To this end, we treat undriven

 $k \neq i$, and $k \neq j$. The power balance (21), valid for an

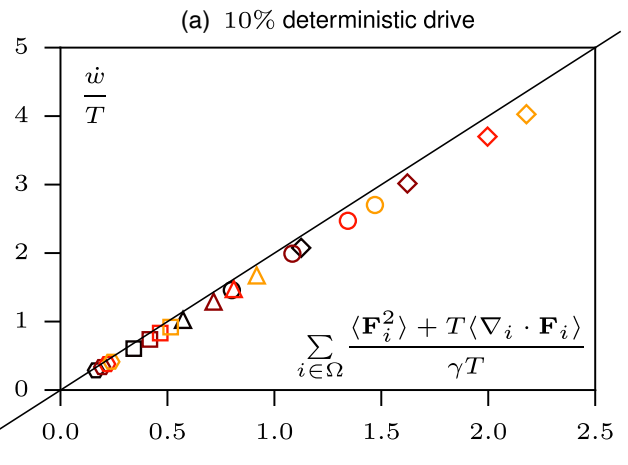
arbitrary driving, either deterministic or active, is our first main result. Importantly, it holds for generic interactions and for any number of driven particles, namely, not only in the limit of dilute tracers, in contrast with the results in Sec.II B.

In practice, it reflects how density correlations adapt to the presence of nonequilibrium forces. For a vanishing rate of work ($\underline{w} \% 0 \% \underline{w}_{act}$), one recovers the first order of the equilibrium Yvon-Born-Green (YBG) hierarchy, in its integral form, for two-componentfluids [90]. At a finite rate of work ($\underline{w} \neq 0$), the relation between the two-body correlation g and the three-body terms fg; ghg is now implicitly constrained by dissipation. A direct implication is that the rate of work can now be inferred simply by measuring static density correlations provided that the pairwise interaction potential is known, for a given driven liquid. Importantly, such an approach does not require any invasive methodsbased on comparing fluctuations and response [54–58], and it does not rely on a detailed analysis of particle trajectories [60,61] or currents in phase space [59,62], whose experimental mplementation can require elaborate techniques [3,4].

However, the power balance (21) is not straightforward to test, either numerically or experimentally, due to the three-body correlations an equilibrium, where tracer and bath particles are indistinguishable, we get $g_{3a} \frac{1}{4} g_{3b}$. Assuming thatthis result remains approximately valid in the driven case for a smalfraction of tracers the rate of work can simply be written in terms of the force exerted on a tracer $F_i \frac{1}{4} - \prod_i \nabla_i v \delta r_i - r_j \triangleright$ as

To probe the validity of this result, we simulate the dynamics (1) where 10% of particles are subject to the driving force, considering either the deterministic periodic Appendix A. Parameters Pe 1/4 12 (hexagons), 18 (square), drive (2) or the active noise drive (3). Interactions are set by the Weeks-Chandler-Andersen potentialor 1/4 $4v_0\frac{1}{2}\delta\sigma = jrj \not = -\delta\sigma = jrj \not = 0$ ments in Fig. 2 show that Eq. (23) is indeed a good approximation at small Pe and small namely, when the drive only weakly perturbs the liquid. The discrepancy is higher for the active case compared with the deterministic contribution in the power balance (21) we focus on the one, since vact ¼ 0 in the latter without any approximation. observable I ¼ ½ ð∇√2 T∇ ² vðg − g_{eq}Þ. At a given τ, prospecting the whole system, our results demonstrate that master curve for our numerical range $Pe \in \frac{1}{2}12$; 36as the rate of work can actually be evaluated with only a small ported in the middle column in Fig. error by considering solely forces acting on tracer:The small fraction of driven tracers.

by dissipation, we measure the deviation from equilibrium the rate of work also scales like Pe2, it suggests the pair correlationsg - g_{eq} due to the driving forces (left column in Fig. 3). In particular, inspired by the two-body



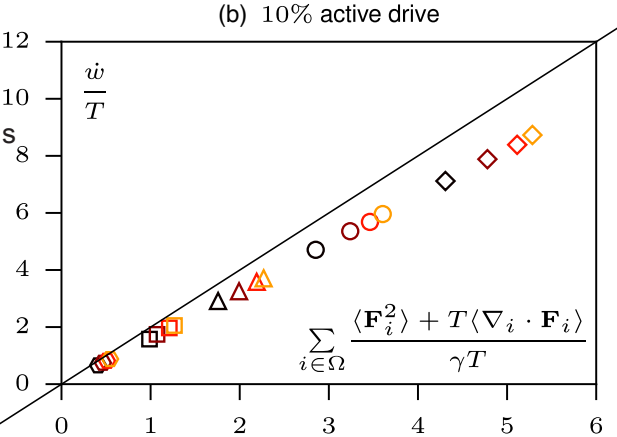


FIG. 2. Parametric plotof the gate of work \underline{w} =T and of the statistics of bath-tracerforces $_{i\in\Omega}$ 1/2 h $^{fi}_{i}$ b Th $\nabla_{i}\cdot F_{i}$ i= $\delta\gamma$ Tb when 10% of particles are driven by either (a) a deterministic force or (b) an active force. The solid line with slope 2 refers to the approximate relation (23). The satisfying agreement with numerical data indicates that the rate of work can be estimated by only measuring bath-tracer forces. The simulations are performed with N 1/4 4500 particles using the procedure described in 24 (triangle), 30 (circle), and 36 (diamond); (a) $\tau T = \delta \gamma \sigma^2 P^{-1/4}$ 2×10^{-1} (black), 3×10^{1} (brown), 4×10^{1} (red), and 5×10^{1} (orange);(b) $\tau T = \delta \gamma \sigma^2 P^{1/4} 2 \times 10^2$ (black), 3×10^{-2} (brown), 4×10^{-2} (red), and 5×10^{2} (orange).

In contrast to previous approaches [3,54,92], which rely oscaling I by Pe reveals that all curves almost collapse into 3. In practice, particles overlap more for a stronger drive, so that g departs contribution of forces on other particles is negligible for a from zero at a smaller interparticle distance. To correct for this aspect, we introduce a shift of the curves I ðiriÞ as To evaluate further the change in liquid structure induce in jrj þ a, where að PeÞ is a fitting parameter. Given that existence of an underlying relation between and w. In practice, a linear fitting provides a satisfactory

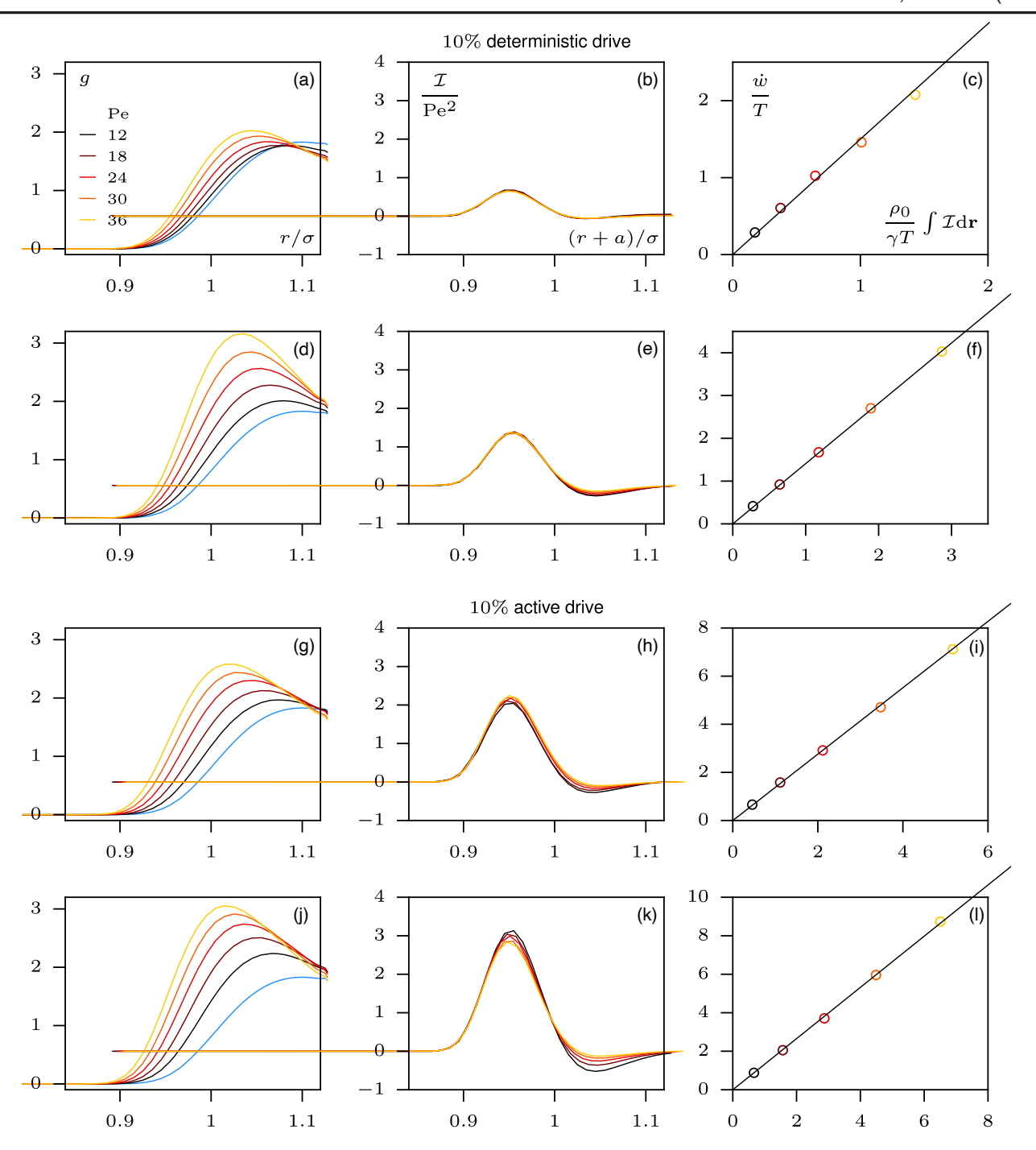


FIG. 3. Connecting dissipation and structure for a liquid where 10% of particles are driven by either deterministic or active forces. (Left) Bath-tracer density correlation g as a function of interparticle distance $r=\sigma$. The blue solid line corresponds to the equilibrium correlation function g for Pe $\frac{1}{4}$ 0. (Middle) Deviation from equilibrium correlations I $\frac{1}{4}$ $\frac{1}{$

agreement between them, as shown in the right column irfor explicit predictions on the emerging structure. Fig. 3:

$$\underline{w} \ ^{1/4} \frac{\alpha \rho_0}{v} \ ^{1/2} g \tilde{o} r \dot{p} - \underline{\phi} \tilde{o} r \dot{p} f \frac{1}{2} \nabla v \tilde{o} r \dot{p}^2 - T \nabla^2 v \tilde{o} r \dot{p} g dr; \ \tilde{o} 24 \dot{p} dr \dot{p} d$$

where α is a fitting parameter independent the Péclet number. This empirical relation demonstrates that the limit of dilute tracers, the rate of work can actually be directly estimated by comparing driven and equilibrium pair correlations for both deterministic and active drives. Comparing Eqs.(21) and (24), we deduce the following integral relation between density correlations:

Interestingly, it is reminiscent again of the connection between density correlations provided by the YBG hierarchy at equilibrium [90]. Similarly, the relation (25) amounts to a constraint on density correlations, now valid difference is that Eq. (27) features interaction forces \(\psi \) for nonequilibrium liquids, which could guide the search

Importantly, it does not rely on any equilibrium mapping, in contrast to previous works [93-95], since it remains valid for non-negligible dissipation.

The power balance (21) can actually be extended to the case where albarticles in the liquid are driven as

where g and gnow refer, respectively, to the two-body and three-body density correlations among abarticles. This extension leads to an exactelation between the rate of work and the forces applied to particles, Fas

$$\underline{\mathbf{w}} \stackrel{1}{\cancel{4}} \frac{\mathbf{X}}{\mathbf{Y}} \stackrel{1}{\cancel{b}} \stackrel{1}{\cancel{h}} \mathbf{h} \mathbf{h} \nabla_{\mathbf{i}} \cdot \mathbf{F}_{\mathbf{i}} \mathbf{i}; \qquad \tilde{\mathbf{o}} \mathbf{27} \mathbf{b}$$

which differs from the relation (23) for driven tracers by an overall factor of 2. A result analogous to Eq. (27) was found previously for a deterministic drive [36,96]. The main in the rhs, thus allowing one to evaluate the rate of work

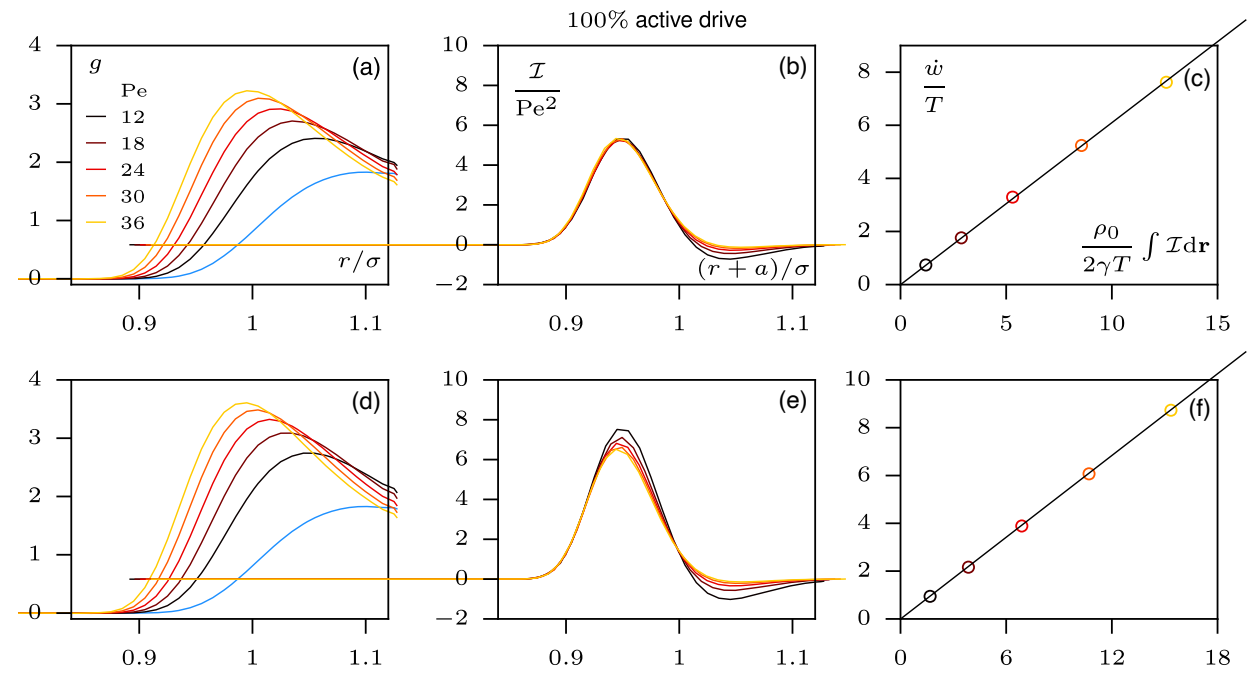


FIG. 4. Connecting dissipation and structure for a liquid where 100% of particles are driven by an active for the ft) Density correlation g as a function of interparticle distance r=σ. The blue solid line corresponds to the equilibrium correlation function g Pe ¼ 0.(Middle) Deviation from equilibrium correlations I ¼ ½δ∇VÞ T∇ 2vðg − g_{eq}Þ scaled by Peas a function of ðr þ aÞ=σ, where að PeÞ is a fitting parameter. The data almost collapse into a master curve for each row, namely, at a given τ. (Right) Parametr plot of the rate of workeT and the integrated deviation from equilibrium correlations δφρdr=δ2γTÞ showing a linear relation. The black solid line with slope α is the best linear fit, and the marker colors refer to the scheme and in the left and right columns. Simulation details are in Appendix AParameters $\pi T = \delta \gamma \sigma^2 P$; $\alpha g \frac{1}{4} f 2 \times 10^2$; 1.22g (a)–(c) and f5 × 10²; 1.14g (d)–(f).

without any prior knowledge on the driving force. Besides and organization in driven systems, which is distinct from it is valid for both deterministic and active drives. Moreover, conducting the same analysis of density correlations as for driven tracers, I exhibits agaig a scaling withthat are conditioned on a nonzero rate of work. In Pe², as reported in Fig. 4. We show threatnd I orbdr are also linearly related. Introducing the linear coefficientas $\alpha \rho_0 = \delta 2 \gamma \text{ Pis consistent with substituting Eq. (25) into$ Eq. (26), where $g_{3;a}
ightarrow g_{3;b}$ is now replaced by $2g_3$. Hence, it demonstrates that the rate of work is also accessible from the nonequilibrium deviation of pair correlations in fully driven liquids.

Overall, the results of this section illustrate how dissipation affects the transportand structural properties of driven liquids, measured in terms ofthe diffusion coefficient and density fluctuations. These findings motivate thenforce a targetondition on the rate of work [98]. following question: Can nonequilibrium forces be tuned to reliably stabilize target configurations? To explore this question, we rely in what follows on the framework of large-deviation theory. In practice, our strategy amounts texp½kt EðsÞds, where E is the observable which conbiasing trajectories in terms of dissipation, related to manylitions the dynamics, e.g., energy flow rate, and κ is a body interactions by Eq.(21), to mimic the effect of an external drive. Following this route, our analytical and numerical results provide some concrete intuition for how controls the average value of E [37]Before deriving the interactions in a multicomponent ystem can be controllably renormalized by nonequilibrium forcesHence, we demonstrate the ability to nucleate structures different frowduce a simple example in which the connection between tion to help guide self-assembly [97] and collective motiorbe clearly seen. [25] far from equilibrium. These results further illustrate the interplay between energy dissipation and organization in

III. INTERACTIONS IN BIASED ENSEMBLES

nonequilibrium many-body settings.

promoted by means of a dynamical bias, we begin by considering a system of interacting Brownian particles without any driving force:

where the statistics of the noise termis the same as the one in Eq. (1). The rate of work \underline{w} defined in Eq. (14) is where $V_{i,j}^{T} = V_{i,j}^{T} = V$ a nonzero rate of energy flow through the system, we consider an explicit driving force Fi, and we explore its effects on the transport and structural properties of the liquid. In practice, different types of driving can lead to the $A_i \frac{1}{4\sqrt{1}} \frac{1}{4\sqrt{$ same dissipation this section, using the framework of the large-deviation theory, we take an alternative approach where the dynamics is now conditioned by enforcing a required energy flow withoutany explicit driving. Thus, exploring how the system adapts to this requirement provides a new insight into the relation between dissipation can also be written as

To this end, we focus on the subset of noise realizations particular, these realizations no longer have a zero average, so that one can redefine the noise term in Eq. (28) as ξ $\xi_i \not F_{aux;i}$ by introducing an auxiliary force $\xi_{ux;i}$ [38,50]. Hence, the stochastic dynamics given by Eq.(28) with added force Eux;i provides an explicit case which ensures a nonzero energy flow rate. In practice, this dynamics can be drastically different from the original one, thus opening the door to stabilizing unexpected structure and to promoting novel collective effects. Interestingly, such a dynamics can actually be regarded as the optimal strategy to effectively

yet complements the approach in Sec.

Formally, to study the dynamics conditioned by dissipation, we bias the probability of trajectories. This biasing is done by introducing an exponential weighting factor conjugate field. In practice, the relative importance of biasing in the dynamics is controlled by κ, which, in turn, central results of this section, namely, relations between biased energy flow rates and organizatione first introthose characteristic of the equilibrium Boltzmann distribu-auxiliary forces and an exponentially biased ensemble can

A. Dvnamical bias and external forces

To introduce pedagogically our methods, we first show how biasing trajectories can lead to effectively introducing a driving force. Inspired by the role of dissipation in To investigate how target structures and dynamics can weerging liquid properties, as discussed in Sec.II, we bias the equilibrium dynamics (28) with the sum of the dissipation and the rate of work, scaled by T, that would be produced by applying a constant force to a subset Ω of particles:

$$E \frac{1}{\sqrt{T}} \frac{X}{\int_{i=0}^{T} F_d \cdot \frac{1}{2} Y_i + \nabla_i V; \qquad \qquad \text{\'o} 29$$

ble is obtained with standard methods [99,100]:

$$A_{i} \frac{1}{4\gamma T} \frac{1}{2\gamma} |p\nabla_{i} V|^{2} - \frac{1}{2\gamma} \nabla_{i}^{2} V - \frac{\kappa}{\gamma T} \delta_{i \in \Omega} F_{d} \cdot \frac{1}{2\gamma} |p\nabla_{i} V;$$
th

$$\delta 30 P$$

where the first two terms correspond to the unbiased dynamics (28) and the third one to the bias in Eq.(29).

As a result, given that the last term in Eq. (31) can be absorbed in a normalization factor, we deduce that the trajectories biased by Eq. (29) can be generated, at leading rticle-based diffusive systems restricted to small bise is applied to every particle in Ω In particular, it does not feature any long-range interactions which are usually found In our case, a simple expression can be obtained for the in auxiliary dynamics [101].

B. Dynamical bias and modified interactions

To go beyond the case of applying a constant force, we now seek for a dynamical bias which regulates particle interactions in a controlled manner. In particular, we examine cases where the control parameters exspecific to particle pairs fi; jg, so that the biasing factor in path probability now reads $\exp^{1}\!\!/_{\!\!2_{i,j}} \; \kappa_{ij} \stackrel{\text{$}^{\uparrow}}{_{0}} E_{ij} \; \tilde{\text{OsPds.}} \; \text{Now, our}$ choice for the biasing function $\boldsymbol{E}_{ij}\;$ is informed by the connection between the rate of work and many-body interactions in driven liquids, as detailed in Sec. II C. Specifically, we observe that the power balance (21) for a deterministic drive ($\underline{w}_{act} \frac{1}{4} 0$) can be written as $\underline{w} \frac{1}{4}$ $_{i \in \Omega;j}$ hLvðr, - r_j Þi in terms of the evolution operator of the equilibrium dynamics (28) defined by VL 1/4 $_{i}\frac{1}{2}T\nabla - \nabla_{i}V \cdot \nabla_{i}$. This observation motivates us to consider the following bias:

$$E_{ij} \frac{1}{4} \frac{1}{4T} Lv \tilde{o} r_i - r_j b$$
: \tilde{o} 32b

In the unbiased ensembles in SedI C, hEi i provides a measure of the rate at which driving forces pump energy into or extract energy from the specific interaction between therefore, biasing with Eq. (32) amounts to changing the the ith and jth particles. Here, instead of driving the system strength of particle interaction by a factor is specifically with a specific driving force, trajectories are driven by atypical realizations of the noise generated by biased sampling.

To explore how this bias modifies interaction by first employ a derivation different from the path integral approach in Sec. III A. Based on the procedure in Refs. [38,50], the auxiliary physical dynamics, which has the same statistical properties as in the biased enser can be constructed by solving the eigenvalue equation

X
L
$$\models$$
 κ_{ij} E_{ij} G \eth fr_kg; κ \trianglerighteq ¼ λ \eth κ \trianglerighteq G \eth (g); κ \trianglerighteq ; \eth 33 \trianglerighteq

where the eigenvalue parametrized by K, is the scaled cumulant-generating function appropriate to. ☐ he auxiliary dynamics is then defined by replacing the interactiomow biasing with Eq. (32). To this end, we consider the potential in Eq. (28) by the following auxiliary potential:

In practice, computing G is a highly nontrivial procedure for many-body systems. The explicit solutions considered so far concern either exclusion processes [66,102,103] or order, in a physical dynamics where the external force 2x regimes [104,105] and noninteracting cases in some specific potentials [106–108].

> auxiliary potentiaN_i by solving Eq. (33) perturbatively at small bias parameter Specifically, we expand

where G is the uniform eigenvector associated with the zero eigenvalueGiven that hE; i ¼ 0 in the steady state, which follows from the vanishing current condition in the unbiased dynamics (h 1/4 0), the leading nontrivial order of Eq. (33) reads

Substituting the explicitexpressions for the biasing function in Eq. (32), we then deduce that $\frac{4}{7}$ $\frac{1}{6}$ - $\frac{1}{6}$ $\frac{$ is a solution of the eigenvalue problem to the order of κ . The auxiliary potential follows as

$$\tilde{V} \frac{1}{2} \frac{1}{i,j} \tilde{d} 1 \not + \kappa_{ij} \not + v \tilde{d} r - r_{j} \not + \tilde{d} 0 \tilde{d} \dot{d} + \tilde{d} 0$$

for any pair fi; jg, which is the main result of this section.

While energy flows are sustained by explicit nonequilibrium forces in Sec. II, we now maintain a nonzero average for Eii by a biased sampling of trajectories. The corresponding noise realizations can be thought of as an external protocol, which leads to modifying the energy landscape sampled by the biased system as given in E(\$7). Note that the tuning interaction strength between targeted pairs is qualitatively consistent with the effect of external driving. Indeed, phase separation in mixtures of driven and undriven particles, reported both experimentally and numerically, can be rationalized in terms of an effective decrease of specific interactions between these particles [21,23].

Moreover, the techniques in Sec. III A allow one to anticipate the trajectories generated laigher order when ensemble where the first-orderdynamics, given by the

potential (37), is biased with exp¹/₂₁ ɛðsÞds defined in terms of

$$\epsilon \frac{1}{4\gamma T} \frac{X}{k} = K_{ij} \nabla_k v \frac{1}{2} \delta s \dot{p} - \dot{p} \delta s \dot{p}^2$$
: $\delta 38 \dot{p}$

As detailed in Appendix C, this ensemble is equivalent to biasing the original dynamics (28) with Eq. (32). Thus, the effect of higher-order bias on trajectories amounts to maximizing the squared forces in the integrand of Eq. (38), which effectively tends to clusterparticles for both signs of κ_i .

Finally, the decomposition between the first-order aux- κ_{ii} $\frac{1}{4}$ $\kappa \delta_{\in \Omega} \delta_{i \in \Omega}$, where all pairs between a subset and iliary potential and higher-ordersymmetric bias can be extended to a generic class of biases of the form TE/4 LAðr_i - r_i Þ for an arbitrary observable A: The correspond_{mmersed} in the liquid, to connect with the settings ing first-order auxiliary potentialV b 2 i:i κ_{ii} Aðr_i - r_i Þ is now complemented with the higher-order bias (38), where A replaces v. Such a bias is reminiscent of, yet

qualitatively different from, the escape rate used to promote dynamical heterogeneity in glassy systems [41,109]. In our case, clustering is favored for both positive and negative bias parameters_{ii}k In particular, this result is in contrast with the emergence of a hyperuniform phase, where largescale fluctuations are suppressed ported when biasing some hydrodynamic theories of diffusive systems [110].

C. Numerical sampling of biased structures

To illustrate the potential of our bias to control liquid properties, we focus in what follows on the specific case other particles are biased with the same strength k. Here, the set Ω could, for instance, refer to some tracer particles in Sec. II.

To confirm numerically the validity of our approach, we first probe the range of the first-order auxiliary dynamics

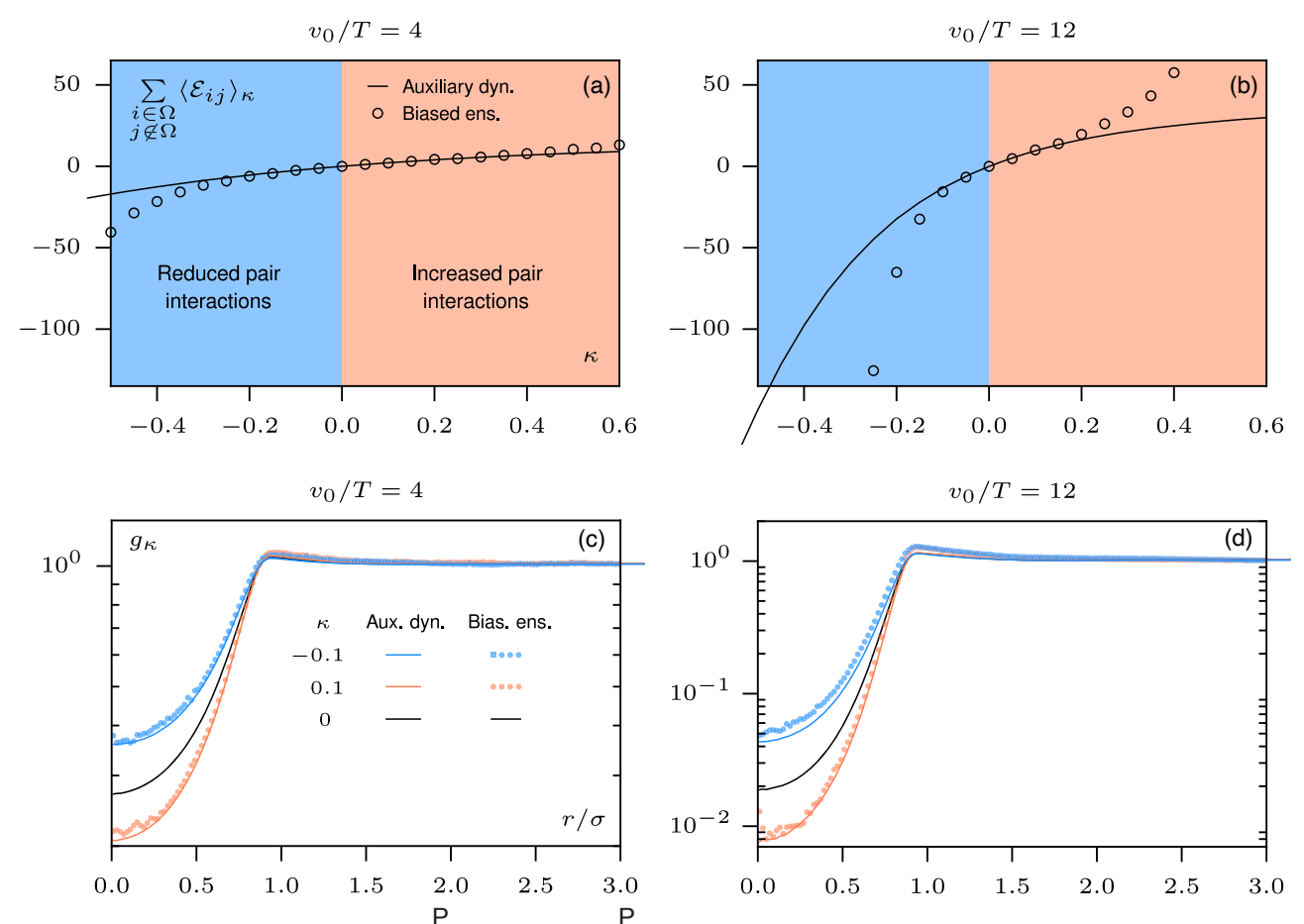


FIG. 5. (a),(b) Average biasing observable $_{\in \Omega; j \notin \Omega}$ hE $_{ij}$ i $_{\kappa}$ $^{\prime}$ $^{\prime}$ $^{\prime}$ $^{\prime}$ $^{\prime}$ $^{\prime}$ $^{\prime}$ $^{\prime}$ $^{\prime}$ $^{\prime}$ i $_{i \in \Omega; j \notin \Omega}$ hLvðr $_{i}$ - r $_{j}$ P $_{k}$ =T as a function of bias parameter κ, where L and v, respectively, denote the evolution operator and the pair potential of the equilibrium dynamics (28). Results from the first-order auxiliary dynamics (solid lines) and from a direct sampling of the biased ensemble (circles) coincide for a finite range of κ. (c),(d) Bias density correlation gas a function of interparticle distance r=o obtained from auxiliary dynamics (solid lines) and direct sampling (dotted lines). At leading order, our dynamical bias effectively renormalizes the potential v by a factor κ for specific pairs of particles fi $\in \Omega$; $j \notin \Omega g$, in satisfying agreement with direct sampling. This renormalization illustrates the control of liquid structure at small κ and weak interaction Simulation details are in Appendix A.

We compare measurements of _i= Ω ; $j \notin \Omega$ h E_{ij} i $_{\kappa}$, where h $\cdot k$ simulations with the renormalized potentials in Eq.(37) and from a direct sampling of the biased ensemble The latter is implemented with a cloning algorithm which regularly selects and multiplies rare realizations foefficient sampling [46,63-68]. For convenience interactions are now given by the soft-core potential vorb 1/4 $v_0 \exp(-1) = \frac{1}{2} - \delta i r i = \frac{1}{2} \Theta \delta \sigma - i r i \Phi$. For weak interbetween the two measurements for a finite range of as reported in Fig. 5(a), which supports the validity of our perturbation up to an interaction change between -20% and $\phi 40\%$. The range of validity decreases as $v_0 = T$ increases shown in Fig.5(b), and we expect a similar trend when also increasing the number of biased pairs.

we now compare the density correlations of biased pairs $g_{k} \tilde{o} r \triangleright \sim \ _{i \in \Omega; j \notin \Omega} \ h \delta \tilde{o} r - \mathfrak{r} \not \triangleright \mathfrak{r}_{i} \not \triangleright \mathfrak{t}_{k} \quad obtained \ from \ both$ direct sampling and first-order auxiliary dynamics. For $\kappa \frac{1}{4}$ 0.1, we observe that the structural modification induced by the bias becomes more dramatic as v_0 =T increases. The agreement between the cloning and auxiliary Ω (not in Ω), which, in turn, dynamics is good for the whole curve when $v_0=T \frac{1}{4} 4$, whereas a deviation appears beyond $r \approx \sigma$ when the region of particle overlap $r < \sigma$ is well reproduced. These results corroborate the ability of the first-order auxiliary dynamics to capture interaction changes as a simple renormalization of the potential strength. In contrast, the tendency for particles to cluster, manifest numerically in the increased peak value at $r \approx \sigma$, is a higher-order As a final illustration of how collective effects can effect missed by this auxiliary dynamics where ₹ 1/4 12.

where interactions are predicted to be simply renormalize that the peak value is comparable for $\kappa \frac{1}{4}$ 0.1, in agreement with Eq. (38) being symmetric in k. Altogether, denotes an average in the biased ensemble, obtained frommese results demonstrate that our bias modulates the liquid structure in a controlled manner for a small bias and weak interactions as predicted by Eq37).

Finally, we probe numerically the effect of a large bias (jκj > 1) using direct sampling to explore configurations significantly distinct from the one of the equilibrium dynamics (28). The particles spontaneously tend to cluster for both positive and negative kas shown in Fig. 6 and actions (y, 1/4 4T), we observe a very satisfying agreement movies in Ref. [73]. This result confirms the propensity of trajectories to maximize interaction forces at a high bias, as captured by Eq. (38). Importantly, the shape of clusters differs depending on the sign of κ: A micellelike structure featuring the particles in Ω at the core (blue) surrounded by others (red) appears for $\kappa \frac{1}{4}$ –3whereas clusters have a random composition fork 1/4 3. Again, this result agrees To explore further the features of this biased ensemble with the renormalized interactions being either increased $(\kappa > 0)$ or decreased $(\kappa < 0)$.In practice, the interaction strength changes sign when $\kappa < -1$ according to Eq. (37), so that the red-blue pairs are effectively attractive for $\kappa \frac{1}{4}$ -3. To optimize the overall energy, the most favorable configuration then consists in maximizing (minimizing) the stabilizes a cluster of blues surrounded by reds. In general, two types of configuration should generically be stabilized v_0 =T ½ 12, as shown in Figs. 5(c) and 5(d). In both cases for a given interaction potential v, depending on the sign of the bias. Overall, this result establishes a reliable proof of principle for the design of tailored self-assembled structures with our specific choice of biased ensembles.

D. Bias-induced collective motion

be controlled by dynamicabias, we consider a modebf

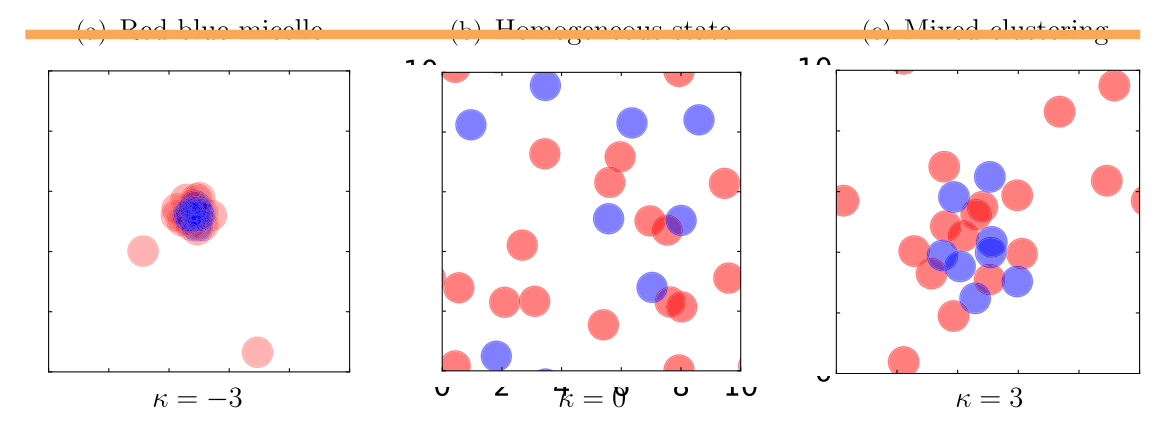


FIG. 6. Configurations obtained from a directampling of the biased ensemble where the pair interactions between red and blue particles are selectively modified. In the unbiased dynamics ($\kappa \% 0$), interactions are purely repulsive with a soft core which has a sim strength for all particles, either red or blue, so that the system is homogeneous. The dynamical bias promotes clustering for both signs κ, yet it changes interaction selectively for either sign. The repulsion is increased between red and blue particles for κ ¼ 3, and their interactions become effectively attractive for κ ¼ –3. As a result, the clusters which emerge spontaneously have different structures: either a random composition of mixed reds and blues ($\kappa \frac{1}{4}$ 3) or a micellelike structure with a blue core ($\kappa \frac{1}{4}$ -3). This result illustrates how biasing specific pairs leads to supervised spatial anization Simulation details are in Appendix A and movies in Ref. 3].

self-propelled particles where interactions are now medi- the corresponding hydrodynamic equations redicts the ated only via the angular dynamics [69]:

where V₀ denotes the self-propulsion velocity, uδθÞ 1/4 δcos θ; sin θÞ is the unitector, and μ_r is the rotational δcos θ; sin θÞ is the univector, and μ_r is the rotational mobility. The term η is a zero-mean Gaussian white noise $E_\theta \frac{1}{4} - \frac{1}{2} \frac{\partial}{\partial \theta_i} b \frac{\mu_r}{D_r} \frac{X}{k} T δθ - θ_k$; $r_i - r_k b$ with correlations brother 2Dδ. δδtb given in terms with correlations h_i δt Þηδ0 Þi ¼ 2 ρδ_i δ δt Þ given in terms of the rotational diffusion coefficient D_r. To promote alignment between neighboring particleswe choose the pairwise torque as T δθ; rÞ ¼ Θδσ − jrjÞ sin θ²lðπīσhis dynamics was originally introduced as a generalization of $\theta = \theta_i \neq 0$ of $\theta = i = r_i \neq 0$, which vanishes in the the Vicsek model to continuous time [25]. Thus, it exhibits teady state. Then, following the procedure detailed in a transition between a isotropic state for smallensity A and large noise Dand a polar state for large densityand small noise D. In practice, the linear stability analysis of

transition to occur when $2D_r \frac{1}{4} \mu_r \rho_0$ [69]. In what follows, our aim is to show that such a transition can also be mediated by tuning interactions with a dynamical bias.

To this end, we take the biasing factor in path probability as $exp\frac{1}{2}$ of E₀0sPds, where the biasing observable E

The average value has proportional to dd=dtb Sec. III B, we deduce that biasing the dynamics (39) with E₀ amounts to considering renormalized interactions of the form

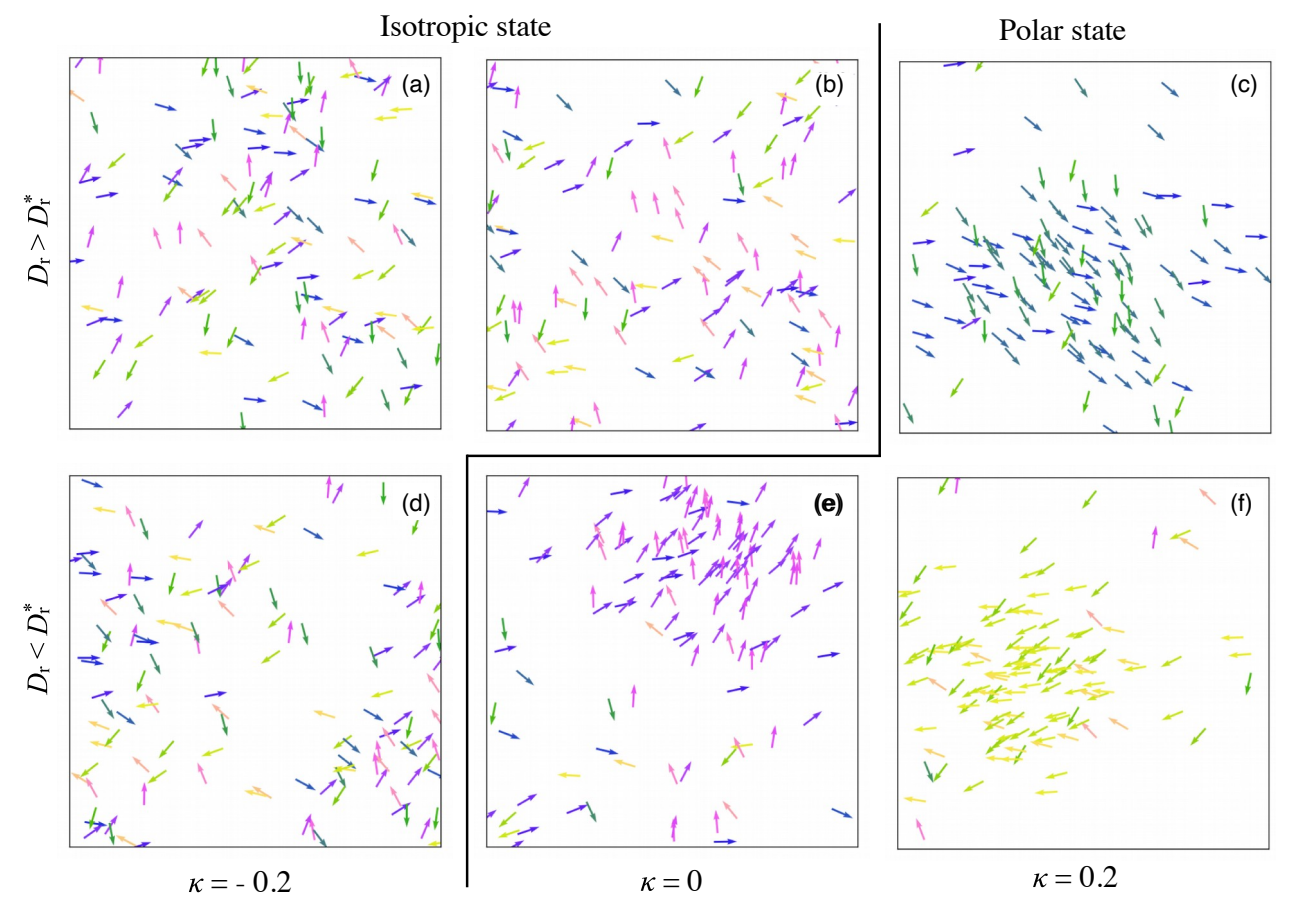


FIG. 7. Configurations obtained from a direct sampling of the biased ensemble for aligning self-propelled particles. The color code refers to the orientation of particles. In the unbiased dynamics ($\kappa \frac{1}{4}$ 0), we observe isotropic and polar states, respectively, at large no (D_r > D_r) and small noise (D< D_r). Here, the critical noise is D¼ 8, and we take the noise values √D7; 9g for, respectively, the polar and isotropic regimes. The dynamical bias leads to renormalizing interactions in a controlled manner, which effectively changes the transition threshold as Đ D rð1 þ κÞ at leading order. As a result, one can stabilize either isotropic or polar states, respectively, for κ < 0 and κ > 0, thus illustrating the ability to trigger or inhibit collective effects in nonequilibrium systems. Simulation details are in Appendix A and movies in Ref[73].

\tilde{T} ¼ ð1 þ kÞT þ Oðk²Þ: ð41Þ

Thus, by promoting a nonzero average for E₀, aligning interactions can be tuned in a controlled manneat first order in k. A higher-order bias leads to maximizing the squared torqueas presented in Appendix C.

We test this prediction numerically using a direct sampling of biased trajectories. We consider values of fD_r; μ ; ρ_0 g above and below the threshold_rD/₄ $\mu_r \rho_0$ =2, the unbiased dynamics ($\kappa \frac{1}{4} 0$), as shown in Fig. Specifically, when the original system is isotropic $(D_r > D_r)$, we observe a transition to polar for $\kappa > 0$, and, conversely, when it is polar (BD,), a transition to isotropic for κ < 0. This observation confirms our result (41), where the bias amounts to changing the angular mobility as $\tilde{\mu}_r$ ¼ δ 1 b κ Þ μ b O δ κ 2 Þ for weak κ , so that the in a controlled manner. linear instability is either triggered or suppressed by solely tuning κ, all other parameters being held the samehus, these results demonstrate how biasing the dynamics with provides useful insights on how to promote atypical appropriate observable leads to control of the emergence on figurations with an external drive. In practice, the spontaneous organizatiowith potential interest for other nonequilibrium dynamics.

IV. CONCLUSION

Developing techniques to characterize and contr**t**e a central and outstanding problem. Despite the apparently o promote the spontaneousself-assembly of complex complex interplay between internal dissipation and emerg_{structures} at the cost of energy dissipation. For instance, ing properties, we demonstrate thattracer diffusion and density correlations can simply be connected to dissipation our approach to design energetic landscapes terms of in driven liquids. We also construct mapping between deterministic and active drives for a specific active matter lize some targetmolecules. model, thus showing how our approach can potentially be extended to a broad class of systems. Importantly, our results open promising perspectives to evaluate dissipation lows one to constrain the dynamics and structure of simply from the structure of the system. Inspired by recenturiven liquids. This constraint paves the way towards works [18,111], one could also introduce a map of dissipation, directly related to the statistics of interaction thermostat. Though the corresponding integrated map would not cover the total dissipation, it would already provide insightful information about locations of low and high dissipation with respect to a constant background set by the squared driving amplitude.

In practice, monitoring dissipation with a well-defined parameter remains an open challenge for many-body systems. To this end, biased ensemble enable one to specify the statistics of dissipation by introducing an additional control parameter analogously to the change from a microcanonicalto a canonical ensemble in equiing rare noise realizations which drive the system away from typical behavior, without introducing any driving force. Pioneering works were focused on favoring

dynamical heterogeneities, it hout affecting the structure, of kinetically constrained models [39-43]. Yet, more recent studies show the potential to also modify density correlations in diffusive systems [48,49,112].

Using these large-deviation techniques, we put forward a particular set of biased ensembles which allows one to regulate the liquid structure in a controlled mannerThe explicit form of the bias is motivated by the relations between dissipation and structure that we derive for driven where the system exhibits either isotropic or polar states iliquids. At leading order, any bias in this class simply leads to introducing additional interactions in the dynamics. Furthermore, a higher-order bias systematically constrains the trajectories to favor the formation of clusters. Based on minimal case studies, we sample the biased configurations, using state-of-the-art numerics [46,63–68], to illustrate the ability to stabilize specific structures and collective effects

Since dynamical bias consists in favoring rare noise fluctuations, the corresponding dynamics effectively driving protocol should simply mimic the biased noise realizations. This line of thought has already been exploited for efficient sampling of the biased ensemble [45,65,113,114], where control forces make rare events become typical. Moreover, since our analytic framework encompasses the case of a specific bias for each pair of behavior of systems operating far from equilibrium remains article, it could potentially be regarded as a fruitful route inspired by recentworks [115,116], one might consider the pair-specific bias parameters, hich selectively stabi-

Overall, these results illustrate how specifying the amount of energy dissipated by nonequilibrium forces controlling the emerging properties of such systems by tuning dissipation accurately. It remains to investigate forces, to resolve spatially where energy is released in the whether similar results can be obtained in more complex systems which could, for instance, potentially include anisotropic building blocks such as driven chirabbjects or active liquid crystals [27,117,118].

ACKNOWLEDGMENTS

The authors acknowledge insightful discussions with Michael E. Cates, David Martin, Robert L. Jack, and Vincenzo Vitelli. This work was granted accesso the HPC resources of CINES/TGCC under the allocation 2018-A0042A10457 made by GENCI and of MesoPSL financed librium thermodynamics [38,50], which is done by select- by the Region IIe de France and the project Equip@Meso (reference ANR-10-EQPX-29-01) of the program Investissementsd'Avenir supervised by the Agence Nationale pour la Recherche. S. V. and L. T. were supported by the University of Chicago Materials Research Science and Engineering Center, which is funded by National Science Foundation under Grant No. DMR-1420709. S. V. acknowledges supportrom the Sloan Foundation and startup funds from the University of Chicago. S. V. an conditions. To sample the biased ensemble we use the L. T. acknowledgesupport from the National Science Foundation under Grant No. DMR-1848306. E. F. is supported by an Oppenheimer Research Fellowship from of clones is 200. The time step is $\delta t \frac{1}{4}$ 10, and the total the University of Cambridge and a Junior Research Fellowship from St.Catherine's College.

APPENDIX A: NUMERICAL SIMULATIONS

In Sec. II A, a custom code of molecular dynamics, basedThis Appendix is devoted to the derivation of the on the finite time difference, is used to perform the simulations in a two-dimensionalbox $10^2 \sigma \times 10^2 \sigma$ with periodic boundary conditions. The time step is δt 1/4-10. and the initial condition is homogeneous. Parameter values a particle driven at constant force in Ref[52,53]. To are $\rho_0 \frac{1}{4} 0.7$, T $\frac{1}{4} 0$, $\sqrt{\frac{1}{4}} 1$, f $\frac{1}{4} 3 \times 10^{-2}$, T $\frac{1}{4} 10^3$, $v_0 \frac{1}{4} 5$, n $\frac{1}{4} 10^2$, and $\sigma \frac{1}{4} 1$.

In Secs. II B and II C, numerical simulations of the dynamics (1) are performed using the LAMMPS simulation package in a two-dimensional boxd 10°σ, where σ is the particle diameter, with periodic boundary conditions at average density p 1/4 0.45. Our custom code motion with the finite time difference. It simply utilizes the [99,100]. It can be separated into contributions from the actually implements overdamped Langevin equations of efficient force computation routines that are built as a part free tracer motion and from interactions, respectively, of the molecular dynamics package The system is first relaxed for 10 conjugate gradient descent steps and later equilibrated during 50_T.We evaluate average values over ten independent trajectories with duration 150_T. The density pair correlations are constructed using ten independenttrajectories, each with duration 50 T.We perform error analysis from the independent simulations and obtain negligible errors for all the data in Figs. 2–4. The time step is 5×10^{-4} , and the bin size for computing the pair correlations is 0.01 σ . We perform simulations at other values of the time step f10⁻⁴; 10⁻⁵g and of the bin size $f5 \times 10^{-3}\sigma$; 2 × 10² σ g to confirm that our calculations of the α coefficients are well converged. Parameter values are here D₀ $\frac{1}{4}$ T= γ is the tracer diffusion coefficient the T $\frac{1}{4}$ 1, γ $\frac{1}{4}$ 10 $\frac{1}{6}$, v₀ $\frac{1}{4}$ 1, and σ $\frac{1}{4}$ 1.

In Sec. III C, a custom code of molecular dynamics, simulations in a two-dimensional box $10\sigma \times 10\sigma$ with periodic boundary conditions We bias the pair potential between eight blue particles and 16 red particles. To described in Appendix A in Ref. [65]. The time interval for cloning is $\Delta t \frac{1}{4}$ 10 δt , and the number of clones is 1600. The time step is $\delta t \frac{1}{4} \cdot 10^{-4}$, the initial relaxation time is $10^4\Delta t$, and the total simulation time is $10^6\Delta t$. Parametervalues are T $\frac{1}{4}$ 1, $\frac{1}{4}$ 1, $\frac{1}{4}$ 4 (Fig. 6), and $\sigma \frac{1}{4}$ 1.

In Sec. III D, a custom code of molecular dynamics based on the finite time difference is used to perform the simulations. N 1/4 128 particles are simulated in a twodimensionalbox of size $4\sigma \times 4\sigma$ with periodic boundary cloning algorithm described in Appendix A in Ref. [65]. The time interval for cloning is $\Delta t \frac{1}{4} 10\delta t$, and the number simulation time is $500\Delta t$. Parametervalues are $\frac{1}{4}$ 2. $\mu_r \frac{1}{4} 2$, $\rho_0 \frac{1}{4} 8$, and $\sigma \frac{1}{4} 1$.

APPENDIX B: DISSIPATION AND DIFFUSION

dissipation rate J and the diffusion coefficient D of a driven tracer, as defined in Sec. II. We employ a perturbative treatmentat weak interactions originally introduced this aim, the tracer-bath interaction potential v is scaled by a small dimensionless parameter \ll 1 in what follows. Besides we focus on the regime of dilute tracers that interactions among thereither direct or mediated by the bath, can be safely neglected.

The dynamic action associated with the tracer dynamics (11) and (12) follows from standard path integral methods denoted by A₀ and A_{int}:

absence of interactions (v $\frac{1}{4}$ 0) and $\frac{1}{10}$ is the process conjugated with the tracer position r₀. For weak interbased on the finite time difference, is used to perform the actions $h \ll 1$, any average value can be then expanded in terms of h as h·i $\frac{1}{4}$ h·i h²hA_{int}·i₀ b Oðh⁴b, where h_iiis the average taken with respecto A 0 only. As a result, determining the first correction from interactions in any sample the biased ensemble, we use the cloning algorithmbservable amounts to computing the corresponding average hAnt·i₀.

> Considering the dissipation rate per particle J = N 1/4 $\text{h\underline{r}_0i} \cdot \text{F}_\text{d} \text{, the leading order is} \underline{\text{rh}i}_0 \cdot \text{F}_\text{d} \not\text{1/4} j \text{F}_\text{d}j^2 \text{=} \gamma \not\text{1/4} f^2 \text{=} \gamma,$ and the first correction reads -h2hA_{int}roi₀ · F_d. Given the explicit form of A int in Eq. (B1), the correlations of interest are

ðB6Þ

$$\begin{split} &\text{hr}_0 \tilde{\delta} t \text{b} \frac{1}{2} \bar{q_0} \tilde{\delta} s \text{b} \dot{e}^{i \cdot \frac{1}{2} \tilde{\delta} \tilde{\delta} s \text{b} - \delta} \tilde{\delta}^{ub} i_0 \\ & \text{14} & \text{iq} \tilde{\delta} \tilde{\delta} t - s \text{b} \bar{e}^{D_0 j q j^2} \tilde{\delta} t - u \text{b} p \tilde{\delta} i q = \gamma \text{b} \cdot \frac{1}{u} F_d \tilde{\delta}^{wb} dw, \\ & \text{hr}_0 \tilde{\delta} t \text{b} \bar{f_0} \tilde{\delta} u \text{b} \bar{r_0} \tilde{\delta} s \text{b} \dot{e}^{i q \cdot \frac{1}{2} \delta} \tilde{\delta}^{sb} - \delta^{\tilde{\delta} ub} i_0 \\ & \text{14} & -\text{iq} \tilde{\delta} \tilde{\delta} t - s \text{b} \bar{e}^{D_0 j q j^2} \tilde{\delta} t - u \text{b} p \tilde{\delta} i q = \gamma \text{b} \cdot \frac{1}{u} F_d \tilde{\delta}^{wb} dw, \end{split}$$

$$\tilde{\delta} B 2 \text{b}$$

For the case of active drive with correlations (3), we exploit the equivalence with a disordered drive detailed in Sec. II A. Substituting the explicit drive (4) in Eq. (B4) and then averaging over disorder in the limit of many oscillators (n \gg 1),we get

where we use that the tracer statistics is Gaussian in the absence of interactions, following Refs. [52,53]. From this $\int_{J-f}^{2} -\frac{N\delta hfb^{2}}{d\gamma^{3}} \frac{dqd\omega^{0}}{dq^{3}} \frac{jqj^{4}jv\delta qb^{2}j\delta\omega^{0}b}{\delta^{2}\pi^{b}^{1}jqj^{4}\omega^{0}b} \frac{dqd\omega^{0}}{\delta^{2}\pi^{b}^{1}jqj^{4}\omega^{0}b} \frac{jqj^{4}jv\delta qb^{2}j\delta\omega^{0}b}{\delta^{2}\pi^{b}^{1}jqj^{4}\omega^{0}b}$

$$\begin{array}{ll} J-f & ^2=\gamma \stackrel{1/N}{\stackrel{N}{\stackrel{N}{\stackrel{D}{\stackrel{O}{=}}}} Z} \frac{dq}{\delta 2\pi P} iq \cdot F_d \delta t Pjq ^2 j v \delta q P^2 \frac{D_0 \not D_G K \delta q P}{D_0 K \delta q P} \\ & \times \int_{-\infty}^{\infty} du e^{-jqj} ^{2} \mathcal{I}_2 \not D D_G K \delta q P \delta t -u Pp \delta iq = \gamma P \cdot \frac{1}{u} F_d \delta w P dw} \\ & \not D O \delta h^4 P; & \delta B 3 P \delta h^4 P \delta t P \delta h^4 P \delta h^4$$

where φð dÞ ¼ 2τ=½1 þ ð tb², yielding

 $\times \frac{D_0 \not\models D_G K \delta q \not\models}{D_G K \delta q \not\models} \not\models O \delta h^4; f^4 \not\models;$

where we use $v_S / v_A = \rho_0$ and $D_G / v_A = \rho_0$. Expanding at small f, we deduce

$$\begin{split} J-f^{2}=&\gamma \frac{1}{4} \frac{N\tau \delta h f \dot{P}^{2}}{d\gamma^{3}} \frac{dq}{\delta 2\pi \dot{P}} \frac{jqj^{2}jv\delta q \dot{P}_{f}^{2}}{\delta 2\pi \dot{P}} \\ &\times \frac{1}{\tau jqj^{2} \frac{1}{2}Q\dot{P}D_{G}K\delta q \dot{P} \dot{P}} \frac{1}{\dot{P}O\delta h^{4}; f^{4}\dot{P}} : \quad \dot{\delta}B7\dot{P} \end{split}$$

Substituting the explicit expression of the deterministic presented in Sec.II B drive (2) in Eq. (B4) and then integrating over u and w, we drives, follow directly.

$$\begin{split} J - f^{2} = & \gamma \frac{1}{4} \frac{N \delta h f b^{2}}{d \gamma^{3}} \frac{Z}{\delta 2 \pi b^{2} j q j^{4} j^{2} \delta p b^{2}} \frac{dq}{\delta 2 \pi b^{2} j q j^{4} j^{2} \delta p b} \frac{1}{G} K \delta q b^{2} b \omega^{2} \\ & \times \frac{D_{0} b D}{D_{0} K \delta q b} b O \delta h^{4}; f^{4} b : \qquad \delta B 5 b \delta b \delta h^{4} \delta q b^{2} \delta h^{4} \delta q b^{2} \delta h^{4} \delta h^$$

The asymptotic results for the rate of work/4 f²=γ - J, presented in Sec.II B for both deterministic and active drives, follow directly.

We now turn to deriving the diffusion coefficient D. It is defined in terms of the mean-squared displacement (MSD) $h\Delta r_0^2 \delta t \text{Pi} \frac{1}{4} h \frac{1}{2} \delta t \text{Pi} - r_0 \delta t \text{Pi} \text{ as D } \frac{1}{4} \lim_{t \to \infty} h\Delta r_0^2 \delta t \text{Pi} = 2 dt.$ At leading order, the MSD reads $h\Delta_0^2 \delta t \text{Pi} \frac{1}{4} 2 dD_0 t.$ To obtain the first order, we need to compute the following correlations:

where we use again that A is Gaussian in terms $o\overline{f}_0$, yielding

$$\begin{split} h\Delta r_0^2 \delta t & \text{Pi} - 2d D_0 t \text{ 1/4} \frac{2h^2}{\gamma^2} \frac{Z}{\delta 2\pi^{\frac{1}{p}}} \frac{dq}{\delta 2\pi^{\frac{1}{p}}} \frac{jqj^2 jv \delta q P_0^2}{K \delta q P} \frac{Z}{\delta s} \frac{ds}{R} \frac{ds}{$$

Expanding at smalf, we get

$$\begin{split} h\Delta r_0^2 \delta t \dot{\triangleright} i - 2 d D_{eq} t \not\!\!\!/_4 - \frac{2 h^2}{V^4} & \frac{dq}{\delta 2 \pi \dot{P}} \frac{j q j^4 j v \delta q \dot{\triangleright}_J^2}{K \delta q \dot{\triangleright}_Z} & \frac{Z}{-\infty} ds \\ & \times e^{-j q j^2 /\!\!\!/_2 Q \dot{\triangleright} D} \, _G K \delta q \dot{\triangleright}_{\delta S - u \dot{\triangleright}} & s \\ & dw_1 dw_2 F_d \delta w_1 \dot{\triangleright} \cdot F_d \delta w_2 \dot{\triangleright} \dot{\triangleright} D \, _G K \delta q \dot{\triangleright}_S \dot{\wedge} S + u \dot{\triangleright} D \, _G K \delta q \dot{\wedge}_S \dot{\wedge}_S$$

where D_{eq} refers to the diffusion coefficient in the absence of driving force (f ½ 0). For the deterministic drive (2), the explicit time integrations give

$$D - D_{eq} \frac{1}{4} \frac{\eth h f \dot{P}^2}{d \gamma^4} \frac{Z}{\eth 2\pi \dot{P} K \eth q \dot{P} \frac{1}{4} \dot{P} D_G K \eth q \dot{P}}{\eth 2\pi \dot{P} K \eth q \dot{P} \frac{1}{4} \dot{P} D_G K \eth q \dot{P}} \times \frac{5jqj^4 \frac{1}{2} \dot{Q} \dot{P} D_G K \eth q \dot{P}^2 \dot{P} \omega^2}{fjqj^4 \frac{1}{2} \dot{Q} \dot{P} D_G K \eth q \dot{P}^2 \dot{P} \omega^2 \dot{Q}^2}$$

$$b O \ddot{D} \dot{P}^4 : f^4 \dot{P} :$$

Using the mapping in Sec. II A for the case of active drive with correlations (3),we deduce

$$\begin{split} D &= D_{eq} \, \frac{1}{4} \, \frac{\eth h f P^2}{d \gamma^4} \, \frac{Z}{\eth 2 \pi P^3} \frac{d q d \omega^0}{\delta 2 \pi P^3} \frac{j q j^2 j v \eth q P_f^2 \varphi \eth \omega P}{K \eth q P \, \frac{1}{4} Q p} \, D_G K \eth q P \\ & \times \frac{5 j q j^4 \frac{1}{2} Q p}{f j q j^4 \frac{1}{2} Q p} \, D_G K \eth q P^2 p \, \delta \omega^0 P^2}{j q j^4 \frac{1}{2} Q p} \, D_G K \delta q P^2 p \, \delta \omega^0 P^2 g^2} \\ & \qquad \qquad p \, O \, \delta h^4; \, f^4 P; \end{split}$$

where again φδθ 1/4 2τ=1/21 þ δπθ, yielding

$$\begin{split} D - D_{eq} \frac{1}{4} \frac{ \tau \delta h f \dot{P}^2}{d \dot{\gamma}^4} & \frac{dq}{\delta 2 \pi \dot{P}} \frac{j v \delta q \dot{P}_f^2}{\delta 2 \pi \dot{P}} K \delta q \dot{P} \frac{1}{4} \dot{Q} \dot{p} D_G K \delta q \dot{P}^2 \\ & \times \frac{5 \tau j q j^2 \frac{1}{2} \dot{Q} \dot{p} D_G K \delta q \dot{P} \dot{p} 3}{f \tau j q j^2 \frac{1}{2} \dot{Q} \dot{p} D_G K \delta q \dot{P} \dot{p} 1 g^2} \\ & \dot{p} O \delta h^4; f^4 \dot{P}: & \delta B 13 \dot{P} \end{split}$$

Finally, we obtain the expressions in the asymptotic regimes, as reported in Sec. II B for both deterministic and active drives.

APPENDIX C: EQUIVALENCE OF BIASED ENSEMBLES

In this Appendix, we demonstrate the equivalence between specific dynamicabiased ensembles First, we considerensembles related to the equilibrium dynamics (28) Ensemble (a) corresponds to biasing with the factor $\exp^{1/2}$ i,j K_{ij} ${}^{t}_{0}$ E_{ij} δ SPds in the path probabilitywhere

$$E_{ij} \frac{1}{\sqrt{T}} \frac{X}{k} \frac{1}{\sqrt{T}} - \nabla_k V \cdot \nabla_k A \delta r_i - r_j b$$
: $\delta C1b$

Ensemble (b) is associated with the first-orderauxiliary dynamics, whose potential reads V \not 2 $_{i;j}$ κ_{ij} $A\delta r_i - r_j \not$ biased with $exp^{1/2} \epsilon^{0} \delta s \not$ where

Obtaining the equivalence between (a) and (b) amounts to showing that their path probabilities are similar. The corresponding dynamic actions, denoted by A **The Corresponding dynamic actions dynamic

and

ðB11Þ

ðB12Þ

$$A_{k}^{\delta b \triangleright} \frac{1}{4\gamma T} | \gamma \underline{r}_{k} \triangleright \nabla_{k} V \triangleright 2 | X | \kappa_{ij} \nabla_{k} A \delta r_{i} - r_{j} \triangleright^{2}$$

$$- \frac{1}{2\gamma} \nabla_{k}^{2} | V \triangleright 2 | X | \kappa_{ij} | A \delta r_{i} - r_{j} \triangleright$$

$$- \frac{1}{\gamma T} | X | \kappa_{ij} | \nabla_{k} A \delta r_{i} - r_{j} \triangleright^{2} : \delta C 4 \triangleright$$

Expanding $A_k^{\bar{o}b\bar{b}}$ in Eq. (C4) and comparing with $A_k^{\bar{o}b\bar{b}}$ in Eq. (C3), it appears that $A_k^{\bar{o}b\bar{b}}$ are indeed equal up to a boundary term proportional to $A_{i;j}^{\bar{o}b\bar{b}}$ in Eq. (C3), it appears that $A_k^{\bar{o}b\bar{b}}$ and $A_k^{\bar{o}b\bar{b}}$ are indeed equal up to a boundary term proportional to $A_{i;j}^{\bar{o}b\bar{b}}$ in Eq. (C3), it appears that $A_k^{\bar{o}b\bar{b}}$ in Eq. (C3), it appears that $A_k^{\bar{o}b\bar{b}}$ in Eq. (C4) and Eq. (C4) and Eq. (C4) and comparing with $A_k^{\bar{o}b\bar{b}}$ in Eq. (C4) and Eq. (C4) and Eq. (C4) and comparing with $A_k^{\bar{o}b\bar{b}}$ in Eq. (C4) and comparing with $A_k^{\bar{o}b\bar{b}}$ in Eq. (C4) and Eq. (C4) and Eq. (C4) and comparing with $A_k^{\bar{o}b\bar{b}}$ in Eq. (C4) and E

We now turn to demonstrate the equivalence between two ensembles related to the Vicsek-like dynamics (39). Ensemble (c) is biased with the factor $\exp \frac{1}{2} k E_{\theta} \delta s P ds$, where E_{θ} is defined in Eq. (40). Ensemble (d) corresponds to the first-order auxiliary dynamics, with the torque given by $\delta 1 \ b \ kPT$ biased with $\exp \frac{1}{2} \epsilon_{\theta} \delta s P ds$, where

$$\epsilon_{\theta} \frac{\sqrt[3]{\delta \kappa \mu} \beta^{2}}{4D_{r}} \frac{X}{\text{i.i.k}} + \sqrt[3]{\delta \theta} - \theta_{k}; r_{i} - r_{k} + \sqrt[3]{\delta \theta} - \theta_{j}; r_{i} - r_{j} + \cdots + \sqrt[3]{\delta \theta} - \theta_{k}; r_{i} - r_{k} + \sqrt[3]{\delta \theta} - \theta_{j}; r_{i} - r_{j} + \cdots + \sqrt[3]{\delta \theta} - \theta_{k}; r_{i} - r_{k} + \sqrt[3]{\delta \theta} - \theta_{k}; r_{i}$$

The dynamic actions for each ensemble, denoted by $B^{\delta\sigma} \delta t P^{1/4} = 0 B_i^{\delta\sigma} \delta P \delta s P ds$ for $\sigma \frac{1}{4}$ fc; dgare given by

$$\begin{split} B_{i}^{\delta c \triangleright} \% & \frac{1}{4D_{r}} \ \theta_{i} - \mu_{r} \overset{X}{\underset{j}{\int}} \ T \ \delta \theta - \theta_{j} \ ; \ r_{i} - r_{j} \ \triangleright^{2} \ \flat \ \frac{\mu_{r}}{2} \frac{\partial}{\partial \theta_{i}} \overset{X}{\underset{j}{\int}} \ T \ \delta \theta - \theta_{j} \ ; \ r_{i} - r_{j} \ \triangleright \\ & \flat \ \frac{\kappa \mu_{r}}{2} \overset{X}{\underset{i}{\partial}} \ \frac{\partial}{\partial \theta_{i}} \ \flat \ \frac{\mu_{r}}{D_{r}} \overset{X}{\underset{k}{\int}} \ T \ \delta \theta - \theta_{k} \ ; \ r_{i} - r_{k} \ \triangleright \ T \ \delta \theta - \theta_{j} \ ; \ r_{i} - r_{j} \ \triangleright \end{split} \qquad \tilde{\delta}C6 \ \triangleright \end{split}$$

and

$$\begin{split} B_{i}^{\delta d \triangleright} \% & \frac{1}{4D_{r}} \theta_{i} - \delta 1 \ \flat \ \kappa \triangleright \mu \sum_{j}^{X} \ T \ \delta \theta_{j} - \theta_{j} \ ; \ r_{i} - r_{j} \ \triangleright^{2} \ \flat \ \frac{\delta 1 \ \flat \ \kappa \triangleright \mu}{2} \frac{\partial}{\partial \theta_{i}} \sum_{j}^{X} \ T \ \delta \theta_{j} - \theta_{j} \ ; \ r_{i} - r_{j} \ \triangleright \\ & - \frac{\delta \kappa \mu \, E^{2}}{4D_{r}} \sum_{i;k}^{X} \ T \ \delta \theta_{j} - \theta_{k} \ ; \ r_{i} - r_{k} \triangleright T \ \delta \theta_{j} - \theta_{j} \ ; \ r_{i} - r_{j} \ \triangleright : \end{split} \qquad \qquad \delta C7 \ \triangleright \end{split}$$

Expanding \Breve{B}^{db} in Eq. (C6) and comparing with \Breve{B}^{dcb} in Eq. (C7), it appears that \Breve{B}^{ddb} and \Breve{B}^{ddb} differ only by a term proportional to $_{i;j}^{\prime}$ θ_{i} T $\delta\theta$ = θ_{j} ; r_{i} = r_{j} \triangleright which can safely be neglected at large t, thus proving the equivalence between ensembles (c) and (d).

- [1] S. Toyabe, T. Okamoto, T. Watanabe-Nakayama-l. Taketani, S. Kudo, and E. Muneyuki, Nonequilibrium Energeticsof a Single f 1-Atpase Molecule, Phys. Rev. Lett. 104, 198103 (2010).
- [2] E. Fodor, W. W. Ahmed, M. Almonacid, M. Bussonnier, N. S. Gov, M.-H. Verlhac, T. Betz, P. Visco, and F. van Wijland, Nonequilibrium Dissipation in Living Oocytes, Europhys.Lett. 116, 30008 (2016).
- [3] C. Battle, C. Broedersz, M. Fakhri, V. Geyer, J. Howard, C. Schmidt, and F. MacKintosh, Broken Detailed Balance at Mesoscopic Scales in Active Biologic Systems Science 352, 604 (2016).
- [4] F. S.Gnesotto, F. Mura, J. Gladrow, and C. PBroedersz, Broken Detailed Balance and Non-Equilibrium Dynamics in Living Systems: A Review, Rep. Prog. Phys. 81, 066601 (2018).
- [5] P. P.Lele, B. G. Hosu, and H. C. Berg, Dynamics of Mechanosensing in the Bacteria Hagellar Motor, Proc. Natl. Acad. Sci. U.S.A. 110, 11839 (2013).
- [6] G. Lan, P. Sartori, S. Neumann, V. Sourjik, and Y. Tu, The Energy-Speed-Accuracy Trade-off in Sensory Adaptation, Nat. Phys. 8, 422 (2012).
- [7] F. Wang, H. Shi, R. He, R. Wang, R. Zhang, and J. Yuan, [23] C. del Junco, L. Tociu, and S. Vaikuntanathan Energy Non-equilibrium Effect in the Allosteric Regulation of the Bacterial Flagellar Switch, Nat. Phys. 13, 710 (2017).
- MacKintosh, and G. H. Koenderink, Active Multistage Coarsening of Actin Networks Driven by Myosin Motors, Proc. Natl. Acad. Sci. U.S.A. 108, 9408 (2011).
- [9] T. Sanchez D. T. N. Chen, S. J. De Camp, M. Heymann, and Z. Dogic, Spontaneous Motion in Hierarchically AssembledActive Matter, Nature (London) 491, 431 (2012).
- [10] L. Blanchoin, R. Boujemaa-Paterski, Sykes, and J. Plastino, Actin Dynamics, Architecture, and Mechanics in [27] B. C. van Zuiden, J. Paulose, W. T. M. Irvine, D. Bartolo, Cell Motility, Physiol. Rev. 94, 235 (2014).
- [11] M. Murrell, P. W.Oakes, M. Lenz, and M. L. Gardel, Forcing Cells into Shape: The Mechanics ofctomyosin Contractility, Nat. Rev. Mol. Cell Biol. 16, 486 (2015).
- [12] S. J. DeCamp, G. S. Redner, A. Baskaran, M. F. Hagan, and Z. Dogic, Orientational Order of Motile Defects in Active NematicsNat. Mater. 14, 1110 (2015).

- [13] M. E. Cates and J.Tailleur, Motility-Induced Phase Separation, Annu. Rev. Condens. Matter Phys. 6, 219 (2015).
- [14] A. P. Solon, Y. Fily, A. Baskaran, M. E. Cates, Y. Kafri, M. Kardar, and J. Tailleur, Pressure Is Not a State Function for Generic Active Fluids Nat. Phys. 11, 673 (2015).
- [15] M. Nguyen and S. Vaikuntanathan, Design Principles for Nonequilibrium Self-AssemblyProc. Natl. Acad. Sci. U.S.A. 113, 14231 (2016).
- [16] É. Fodor, C. Nardini, M. E. Cates, J. Tailleur, P. Visco, and F. van Wijland, How Far from Equilibrium Is Active Matter?, Phys.Rev.Lett. 117, 038103 (2016).
- [17] A. Murugan and S. Vaikuntanathan Topologically Protected Modes in Non-equilibrium Stochastic Systems, Nat. Commun.8, 13881 (2017).
- [18] C. Nardini, É. Fodor, E. Tjhung, F. van Wijland, J. Tailleur, and M. E. Cates, Entropy Production in Field Theories without Time-ReversaSymmetry:Quantifying the Nonequilibrium Character of Active Matter, Phys. Rev. X 7, 021007 (2017).
- [19] M. Nguyen and S. Vaikuntanathan Dissipation Induced Transitions in Elastic StringsarXiv:1803.04368.
- [20] M. C. Marchetti, J. F. Joanny, S. Ramaswamy, T. B. Liverpool, J. Prost, M. Rao, and R. A. Simha, Hydrodynamics of Soft Active MatterRev. Mod. Phys. 85, 1143 (2013).
- [21] M. Han, J. Yan, S. Granick, and E. Luijten, Effective TemperatureConcept Evaluated in an Active Colloid Mixture, Proc. Natl Acad. Sci. U.S.A. 114, 7513 (2017).
- [22] C. Bechinger, R. Di Leonardo, H. Löwen, C. Reichhardt, G. Volpe, and G. Volpe, Active Particles in Complex and Crowded Environments, Rev. Mod. Phys. 88, 045006 (2016).
- Dissipation and Fluctuations in a Driven Liquid, Proc. Natl. Acad. Sci. U.S.A. 115, 3569 (2018).
- [8] M. S. e Silva, M. Depken, B. Stuhrmann, M. Korsten, F. C[24] E. Fodor and M. C.Marchetti, The Statistical Physics of Active Matter: From Self-Catalytic Colloids to Living Cells, Physica (Amsterdam) 504Al,06 (2018).
 - [25] T. Vicsek, A. Czirók, E. Ben-Jacob, I. Cohen, and O. Shochet, Novel Type of Phase Transition in a System of Self-Driven ParticlesPhys.Rev.Lett. 75, 1226 (1995).
 - [26] J. Tailleur and M. E. Cates, Statistical Mechanics of Interacting Run-and-Tumble Bacteria Phys. Rev. Lett. 100, 218103 (2008).
 - and V. Vitelli, Spatiotemporal Order and Emergent Edge Currents in Active Spinner Materials Proc. Natl. Acad. Sci. U.S.A. 113, 12919 (2016).
 - [28] S. C. Takatori and J. F. Brady, Towards a Thermodynamics of Active Matter, Phys. Rev. E 91, 032117 (2015).
 - [29] A. P.Solon, J. Stenhammar, E. Cates, Y. Kafri, and J. Tailleur, Generalized Thermodynamics of Motility-Induced

- Phase Separation: Phase Equilibria, Laplace Pressure, and Change of Ensembles, New J. Phys. 20, 075001 (2018).
- [30] A. P.Solon, J. Stenhammar, M. E. Cates, Y. Kafri, and J. Tailleur, Generalized Thermodynamics Phase Equilibria in Scalar Active Matter, Phys. Rev. E 97, 020602(R)
- [31] T. F. FFarage, P. Krinninger, and J. M. Brader, Effective 91, 042310 (2015).
- [32] R. Wittmann, U. M. B. Marconi, C. Maggi, and J. M. Model for Active Matter II. A Unified Framework for Phase Equilibria, Structure and Mechanica Properties, J. Stat. Mech. 2017, 113208 (2017).
- [33] J. A. McLennan, Statistical Mechanics of the Steady State, Phys.Rev. 115, 1405 (1959).
- [34] T. S. Komatsu and N. Nakagawa, Expression for the Stationary Distribution in Nonequilibrium Steady States, Phys.Rev.Lett. 100.030601 (2008).
- [35] C. Maes, K. Netočný, and B. M. Shergelashvili, Nonequilibrium Relation between Potentialand Stationary Distribution for Driven Diffusion, Phys. Rev. E 80, 011121
- [36] C. Maes and K. Neton, Rigorous Meaning of Mclennan Ensembles J. Math. Phys. (N.Y.) 51, 015219 (2010).
- [37] H. Touchette, The Large Deviation Approach to Statistical Mechanics. Phys. Rep. 478, 1 (2009).
- [38] R. L. Jack and P. Sollich, Large Deviations and Ensembles of Trajectories in Stochastic Models, rog. Theor. Phys. Suppl. 184, 304 (2010).
- [39] J. P.Garrahan, R. L. Jack, V. Lecomte, E. Pitard, K. van Duijvendijk, and F. van Wijland, Dynamical First-Order Phase Transition in Kinetically Constrained Models of GlassesPhys.Rev.Lett. 98, 195702 (2007).
- [40] L. O. Hedges, R. L. Jack, J. P. Garrahan, and D. Chandler, Dynamic Order-Disorder in Atomistic Models of Structural Glass Formers Science 3231309 (2009).
- [41] E. Pitard, V. Lecomte, and F. van Wijland, Dynamic Transition in an Atomic Glass Former: A Molecular-Dynamics Evidence urophys.Lett. 96, 56002 (2011).
- [42] T. Speck, A. Malins, and C. P. Royall, First-Order Phase [60] É. Roldán, J. Barral, P. Martin, J. M. R. Parrondo and F. Transition in a Model Glass Former: Coupling ofLocal Structure and Dynamics, Phys. Rev. Lett. 109, 195703 (2012).
- [43] T. Bodineau, V. Lecomte, and C. Toninelli, Finite Size Scaling of the Dynamical Free-Energy in a Kinetically Constrained Model J. Stat. Phys. 147, 1 (2012).
- Proc. Natl. Acad Sci. U.S.A. 111, 9413 (2014).
- [45] T. Nemoto, R. L. Jack, and V. Lecomte, Finite-Size Scaling of a First-Order Dynamical Phase Transition: Adaptive Population Dynamics and an Effective Model, Phys. Rev. Lett. 118, 115702 (2017).
- [46] J. Tailleur and J. Kurchan, Probing Rare PhysicalTrajectories with Lyapunov Weighted Dynamics, Nat. Phys. 3, 203 (2007).
- [47] T. Laffargue, K.-D. N. Thu-Lam, J. Kurchan, and J. Tailleur, Large Deviations of Lyapunov Exponents, J. Phys. A 46, 254002 (2013).

- [48] F. Cagnetta, F. Corberi, G. Gonnella, and A. Suma, Large Fluctuations and Dynamic Phase Transition in a System of Self-Propelled Particles, Phys. Rev. Lett. 119, 158002 (2017).
- [49] T. Nemoto, É. Fodor, M. E. Cates, R. L. Jack, and J. Tailleur, Optimizing Active Work: Dynamical Phase Transitions, Collective Motion, and Jamming, Phys. Rev. E 99, 022605 (2019).
- Interactions in Active Brownian Suspensions, Phys. Rev. E50] R. Chetrite and H. Touchette, Nonequilibrium Microcanonical and Canonical Ensembles and Their Equivalence, Phys. Rev. Lett. 111, 120601 (2013).
- Brader, Effective Equilibrium States in the Colored-Noise [51] D. S. Dean, Langevin Equation for the Density of a System of Interacting Langevin Processes, Phys.A. 29, L613 (1996).
 - [52] V. Démery and D. S. Dean, Perturbative Path-Integral Study of Active- and Passive-Tracer Diffusion in Fluctuating Fields, Phys. Rev. E 84, 011148 (2011).
 - [53] V. Démery, O. Bénichou, and H. Jacquin, Generalized Langevin Equations for a Driven Tracer in Dense Soft Colloids: Construction and Applications, New J. Phys. 16, 053032 (2014).
 - [54] T. Harada and S.-i. Sasa, Equality Connecting Energy Dissipation with a Violation of the Fluctuation-Response Relation, Phys. Rev. Lett. 95, 130602 (2005).
 - [55] D. Mizuno, C. Tardin, C. F. Schmidt, and F. C. MacKintosh, Nonequilibrium Mechanics of Active Cytoskeletal Networks, Science 315370 (2007).
 - [56] É. Fodor, M. Guo, N. S. Gov, P. Visco, D. A. Weitz, and F. van Wijland, Activity-Driven Fluctuations in Living Cells, Europhys.Lett. 110, 48005 (2015).
 - [57] H. Turlier, D. A. Fedosov, B. Audoly, T. Auth, N. S. Gov, C. Sykes, J.-F. Joanny, G. Gompper, and T. Betz, Equilibrium Physics Breakdown Reveals the Active Nature of Red Blood CellFlickering, Nat. Phys. 12, 513 (2016).
 - [58] W. W.Ahmed, É. Fodor, M. Almonacid, M. Bussonnier, M.-H. Verlhac, N. S. Gov, P. Visco, F. van Wijland, and T. Betz, Active Mechanics Reveal Molecular-Scale Force Kinetics in Living Oocytes, Biophys. J. 114, 1667 (2018).
 - [59] T. R. Gingrich, G. M. Rotskoff, and J. M. Horowitz, Inferring Dissipation from Current Fluctuations, J. Phys. A 50, 184004 (2017).
 - Jülicher, Arrow of Time in Active Fluctuations, arXiv:1803.04743.
 - [61] I. A. Martínez, G. Bisker, J. M. Horowitz, and J. M. R. Parrondo, Inferring Broken Detailed Balance in the Absence of Observable Currents, Nat. Commun. 10, 3542 (2019).
- [44] D. T. Limmer and D. Chandler, Theory of Amorphous Ices[62] J. Li, J. M. Horowitz, T. R. Gingrich, and N. Fakhri, Quantifying Dissipation Using Fluctuating Currents, Nat. Commun. 10, 1666 (2019).
 - [63] C. Giardina, J. Kurchan, and L. Peliti, Direct Evaluation of Large-Deviation FunctionsPhys. Rev. Lett. 96, 120603
 - [64] P. I. Hurtado and P. L. Garrido, Test of the Additivity Principle for Current Fluctuations in a Model of Heat Conduction, Phys. Rev. Lett. 102, 250601 (2009).
 - [65] T. Nemoto, F. Bouchet, R. L. Jack, and V. Lecomte, Population-Dynamics Method with a Multicanonical Feedback ControlPhys.Rev. E 93, 062123 (2016).

- [66] U. Ray, G. Kin-Lic Chan, and D. T. Limmer, Exact Fluctuations of Nonequilibrium Steady States from Approximate Auxiliary Dynamics, Phys. Rev. Lett. 120, 210602 (2018).
- Rare Behavior of Growth Processes via Umbrella Sampling of Trajectories, Phys. Rev. E 97, 032123 (2018).
- [68] T. Brewer, S. R. Clark, R. Bradford, and R. L. Jack, Efficient Characterisation of Large Deviations Using Population Dynamics, J. Stat. Mech. 2018, 053204 (2018).
- [69] F. D. C.Farrell, M. C. Marchetti, D. Marenduzzo and J. Tailleur, Pattern Formation in Self-Propelled Particles with Density-Dependen Motility, Phys. Rev. Lett. 108, 248101 (2012).
- [70] Y. Fily and M. C. Marchetti, Athermal Phase Separation of Self-Propelled Particles with No Alignment Phys. Rev. Lett. 108, 235702 (2012).
- Dynamics of Phase-Separating Active Colloid Iluid. Phys.Rev.Lett. 110, 055701 (2013).
- [72] C. Maggi, U. M. B. Marconi, N. Gnan, and R. Di Leonardo, Multidimensional Stationary Probability Distribution for Interacting Active Particles, Sci. Rep. 5. 10742 (2015).
- [73] See Supplemental Material at http://link.aps.org/ supplemental/10.1103/PhysRevX.9.041026 movies corresponding to Figs1, 6, and 7.
- [74] D. Chandler. Gaussian Field Model of Fluids with an Application to Polymeric Fluids, Phys. Rev. E 48, 2898 (1993).
- [75] M. Krüger and D. S. Dean, A Gaussian Theory for Fluctuations in Simple Liquids, J. Chem. Phys. 146, 134507 (2017).
- [76] V. Démery, Mean-Field Microrheology of a Very Soft Colloidal Suspension: Inertia Induces Shear Thickening, Phys.Rev. E 91, 062301 (2015).
- [77] D. Martin, C. Nardini, M. E. Cates, and É. Fodor, Extracting Maximum Power from Active ColloidaHeat Engines, Europhys. Lett. 121, 60005 (2018).
- [78] V. Démery and É.Fodor, Driven Probe under Harmonic Confinementin a Colloidal Bath, J. Stat. Mech. 2019, 033202 (2019).
- [79] K. Sekimoto, Langevin Equation and Thermodynamics, Prog. Theor. Phys. Suppl. 130, 17 (1998).
- [80] U. Seifert, Stochastic Thermodynamics, Fluctuation Theorems and Molecular Machines, Rep. Prog. Phys. 75, 126001 (2012).
- [81] D. Mandal, K. Klymko, and M. R. DeWeese, Entropy Production and Fluctuation Theorems for Active Matter, Phys.Rev.Lett. 119, 258001 (2017).
- [82] P. Pietzonka and U. Seifert, Entropy Production of Active[101] R. L. Jack and P. Sollich, Effective Interactions and Large Particles and for Particles in Active Baths, J. Phys. A 51, 01LT01 (2018).
- tion and Work Fluctuations in an Ideal Active Gas. Phys. Rev. E 98, 020604(R) (2018).
- [84] L. Dabelow, S. Bo, and R. Eichhorn, Irreversibility in Active Matter Systems: Fluctuation Theorem and Mutual Information, Phys. Rev. X 9, 021009 (2019).

- [85] O. Bénichou, P. Illien, G. Oshanin, A. Sarracino, and R. Voituriez, Nonlinear Response and Emerging Nonequilibrium Microstructures for Biased Diffusion in Confined Crowded Environments, Phys. Rev. E 93, 032128 (2016).
- [67] K. Klymko, P. L. Geissler, J. P. Garrahan, and S. Whitelan [86] E. W. Burkholder and J. F. Brady, Tracer Diffusion in Active Suspension s, hys. Rev. E 95, 052605 (2017).
 - [87] J. StenhammarC. Nardini, R. W. Nash, D. Marenduzzo, and A. Morozov, Role of Correlations in the Collective Behavior of Microswimmer Suspensions, Phys. Rev. Lett. 119,028005 (2017).
 - [88] T. Bertrand, Y. Zhao, O. Bénichou, J. Tailleur, and R. Voituriez, Optimized Diffusion of Run-and-Tumble Particles in Crowded Environments, Phys. Rev. Lett. 120, 198103 (2018).
 - [89] P. Illien, O. Bénichou, G. Oshanin, A. Sarracino and R. Voituriez, Nonequilibrium Fluctuations and Enhanced Diffusion of a Driven Particle in a Dense Environment. Phys.Rev.Lett. 120, 200606 (2018).
- [71] G. S. Redner, M. F. Hagan, and A. Baskaran, Structure ar [90] J.-P. Hansen and I. R. McDonald, Theory of Simple Liquids, 4th ed. (Academic PressOxford, 2013).
 - [91] J. D. Weeks, D. Chandler, and H. C. Andersen, Role of Repulsive Forces in Determining the Equilibrium Structure of Simple Liquids, J. Chem. Phys. 54, 5237 (1971).
 - [92] B. Lander, J. Mehl, V. Blickle, C. Bechinger, and U. Seifert, Noninvasive Measurement of Dissipation in Colloidal SystemsPhys.Rev.E 86, 030401(R) (2012).
 - [93] U. M. B. Marconi and C. Maggi, Towards a Statistical Mechanical Theory of Active Fluids, Soft Matter 11, 8768 (2015).
 - [94] M. Rein and T. Speck, Applicability of Effective Pair Potentials for Active Brownian Particles ur. Phys.J. E 39, 84 (2016).
 - [95] R. Wittmann, C. Maggi, A. Sharma, A. Scacchi, J. M. Brader, and U. M. B. Marconi, Effective Equilibrium States in the Colored-Noise Modefor Active Matter I. Pairwise Forces in the Fox and Unified Colored Noise Approximations J. Stat. Mech. 2017, 113207 (2017).
 - [96] U. Basu, C. Maes, and K. Netočný, Statistical Forces from Close-to-Equilibrium Media, New J. Phys. 17, 115006 (2015).
 - [97] G. Bisker and J. L.England, Nonequilibrium Associative Retrieval of Multiple Stored Self-Assembly Targetsoc. Natl. Acad. Sci. U.S.A. 115, E10531 (2018).
 - [98] R. M. L. Evans, Rules for Transition Rates in Nonequilibrium Steady States, hys. Rev. Lett. 92, 150601 (2004).
 - [99] P. C. Martin, E. D. Siggia, and H. A. Rose, Statistical Dynamics of Classical Systems Phys. Rev. A 8, 423 (1973).
 - [100] C. De Dominicis, A Lagrangian Version of Halperin-Hohenberg-Ma Models for the Dynamics of Critical PhenomenaLett, Nuovo Cimento 12,567 (1975).
 - Deviations in Stochastic Processes ur. Phys. J. Spec. Top. 224, 2351 (2015).
- [83] S. Shankar and M. C. Marchetti, Hidden Entropy Produc-[102] V. Popkov, G. M. Schütz, and D. Simon, ASEP on a Ring Conditioned on Enhanced Flux, J. Stat. Mech. 2010. P10007 (2010).
 - [103] V. Popkov and G. M. Schütz, Transition Probabilities and Dynamic Structure Function in the ASEP Conditioned on Strong Flux, J. Stat. Phys. 142, 627 (2011).

- [104] N. Tizón-Escamilla, V. Lecomte, and E. Bertin, Effective Driven Dynamics for One-Dimensional Conditioned Langevin Processes the Weak-NoiseLimit, J. Stat. Mech. 2019, 013201 (2019).
- [105] K. Proesmans and B. Derrida, Large-Deviation Theory fo[113] T. Brewer, S. R. Clark, R. Bradford, and R. L. Jack, a Brownian Particle on a Ring: A WKB Approach, J. Stat. Mech. 2019, 023201 (2019).
- [106] S. N. Majumdar and A. J. Bray, Large-Deviation Functions for Nonlinear Functionals of a Gaussian Stationary [114] G. Ferré and H. Touchette Adaptive Sampling of Large Markov ProcessPhys.Rev. E 65, 051112 (2002).
- [107] P. T.Nyawo and H. Touchette, Large Deviations of the Current for Driven Periodic Diffusions, PhysRev. E 94, 032101 (2016).
- [108] P. T.Nyawo and H. Touchette, Dynamical Phase Transition in Drifted Brownian Motion, Phys. Rev. E 98, 052103 (2018).
- [109] C. J. Fullerton and R. L. Jack, Dynamical Phase Transitions in Supercooled Liquids: Interpreting Measurements [117] A. Joshi, E. Putzig, A. Baskaran and M. F. Hagan, The of Dynamical Activity, J. Chem. Phys. 138, 224506 (2013).
- [110] R. L. Jack, I. R. Thompson, and P. Sollich, Hyperuniformity and Phase Separation in Biased Ensembles of Trajectories for Diffusive Systems, Phys. Rev. Lett. 114, 06060 [118] N. H. P.Nguyen, D. Klotsa, M. Engel, and S. C.Glotzer, (2015).
- [111] E. Crosato, M. Prokopenko, and R. E. Spinney, Thermodynamics of Emergent Structure in Active MatterarXiv: 1812.08527.

- [112] R. L. Jack and P. Sollich, Large Deviations of the Dynamical Activity in the East Model: Analysing Structure in Biased Trajectories J. Phys. A 47, 015003 (2014).
 - Efficient Characterisation of Large Deviations Using Population Dynamics, J. Stat. Mech. 2018, 053204 (2018).
- Deviations, J. Stat. Phys. 172, 1525 (2018).
- [115] A. Murugan, Z. Zeravcic, M. P. Brenner, and S. Leibler, Multifarious Assembly Mixtures: Systems Allowing Retrievalof Diverse Stored Structure Proc. Natl. Acad. Sci. U.S.A. 112, 54 (2015).
- [116] M. Stern, M. B. Pinson, and A. Murugan, The Complexity of Folding Self-Folding Origami, Phys. Rev.7X 041070 (2017).
 - Interplay between Activity and Filament Flexibility Determines the Emergent Properties of Active Nematics, Soft Matter 15,94 (2019).
 - EmergentCollective Phenomena in a Mixture of Hard Shapesthrough Active Rotation, Phys. Rev. Lett. 112, 075701 (2014).